

AD-A162 433 HAVE MEASUREMENTS ON TRUSS MODEL(U) NEA CAMBRIDGE MA  
J H WILLIAMS ET AL. 01 SEP 85 AFOSR-TR-85-1077  
F49620-83-C-0092

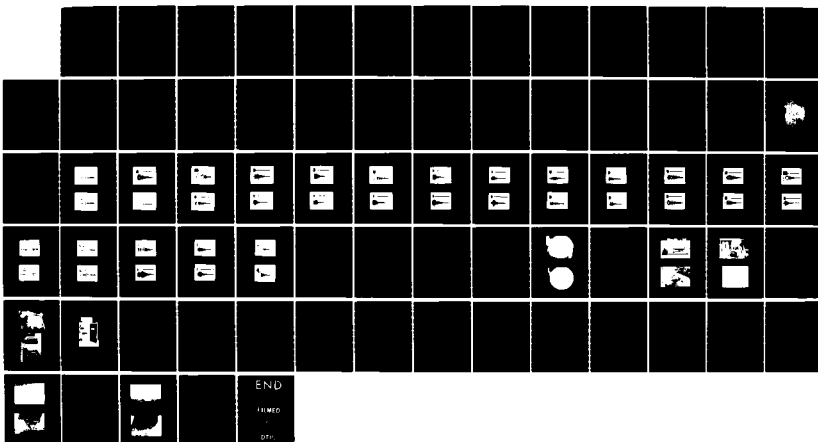
AD-A162 433 HAVE MEASUREMENTS ON TRUSS MODEL(U) NEA CAMBRIDGE MA  
J H WILLIAMS ET AL. 01 SEP 85 AFOSR-TR-85-1077  
F49620-83-C-0092

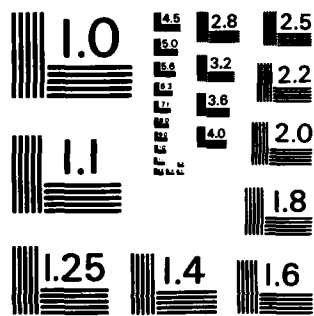
AD-A162 433 HAVE MEASUREMENTS ON TRUSS MODEL(U) NEA CAMBRIDGE MA 1/1  
J H WILLIAMS ET AL. 01 SEP 85 AFOSR-TR-85-1077  
F49620-83-C-0092

UNCLASSIFIED F/G 22/2

UNCLASSIFIED F/G 22/2

UNCLASSIFIED F/G 22/2 NL





MICROCOPY RESOLUTION TEST CHART  
NATIONAL BUREAU OF STANDARDS-1963-A

2

AD-A162 433

CLASSIFIED  
SECURITY CLASSIFICATION OF THIS PAGE

REPORT DOCUMENTATION PAGE

1a. REPORT SECURITY CLASSIFICATION classified			1b. RESTRICTIVE MARKINGS													
2a. SECURITY CLASSIFICATION AUTHORITY			3. DISTRIBUTION/AVAILABILITY OF REPORT Approved for Public Release; Distribution Unlimited.													
4. CLASSIFICATION/DOWNGRADING SCHEDULE			5. MONITORING ORGANIZATION REPORT NUMBER(S) AFOSR-TR. 83-1077													
6a. NAME OF PERFORMING ORGANIZATION WEA		6b. OFFICE SYMBOL (If applicable)	7a. NAME OF MONITORING ORGANIZATION Same as #8													
8a. ADDRESS (City, State and ZIP Code) P.O. Box 260, MIT Branch Cambridge, MA 02139			7b. ADDRESS (City, State and ZIP Code) DTIC ELECTE													
8a. NAME OF FUNDING/SPONSORING ORGANIZATION Air Force Office of Scientific Research		8b. OFFICE SYMBOL (If applicable) AFOSR/NA	9. PROCUREMENT INSTRUMENT IDENTIFICATION NUMBER F49620-83-C-0092													
8c. ADDRESS (City, State and ZIP Code) Bolling AFB, D.C. 20332			10. SOURCE OF FUNDING NOS. <table border="1"><tr><th>PROGRAM ELEMENT NO.</th><th>PROJECT NO.</th><th>TASK NO.</th><th>WORK UNIT NO.</th></tr><tr><td>61102F</td><td>2307</td><td>B1</td><td></td></tr></table>		PROGRAM ELEMENT NO.	PROJECT NO.	TASK NO.	WORK UNIT NO.	61102F	2307	B1					
PROGRAM ELEMENT NO.	PROJECT NO.	TASK NO.	WORK UNIT NO.													
61102F	2307	B1														
11. TITLE (Include Security Classification) Wave Measurements on Truss Model (Unclassified)																
12. PERSONAL AUTHOR(S) James H. Williams, Jr., Howard L. Ou and Samson S. Lee																
13a. TYPE OF REPORT Technical		13b. TIME COVERED FROM 1 Jan 84 to 1 Sept 85	14. DATE OF REPORT (Yr., Mo., Day) 85, Sept. 1	15. PAGE COUNT 72												
16. SUPPLEMENTARY NOTATION																
17. COSATI CODES <table border="1"><tr><th>FIELD</th><th>GROUP</th><th>SUB. GR.</th></tr><tr><td></td><td></td><td></td></tr><tr><td></td><td></td><td></td></tr><tr><td></td><td></td><td></td></tr></table>			FIELD	GROUP	SUB. GR.										18. SUBJECT TERMS (Continue on reverse if necessary and identify by block number) Wave Propagation      Lattice Structures Lattice Models      Large Space Structures	
FIELD	GROUP	SUB. GR.														
19. ABSTRACT (Continue on reverse if necessary and identify by block number) <p>Large space structures (LSS) are large periodic lattice structures being considered for space applications in earth orbit. The vibration and wave propagation characteristics of these structures can affect their performance, integrity and the ability to nondestructively assess that integrity.</p> <p>In this preliminary study, the wave propagation characteristics of a tetrahedral truss model consisting of fiberglass reinforced composite rods and aluminum joints are observed experimentally. Longitudinal ultrasonic transducers are coupled to the joints of the truss model. The input signal consists of a gated sinusoid having a center frequency of 280 kHz. Because a tetrahedral truss, a commonly proposed LSS configuration, can be constructed from basic repeating units of tetrahedrons and pyramids, only tetrahedrons and pyramids are considered.</p> <p>Tetrahedrons and pyramids are constructed by inserting fiberglass reinforced</p>																
20. DISTRIBUTION/AVAILABILITY OF ABSTRACT UNCLASSIFIED/UNLIMITED <input checked="" type="checkbox"/> SAME AS RPT. <input type="checkbox"/> DTIC USERS <input type="checkbox"/>			21. ABSTRACT SECURITY CLASSIFICATION Unclassified													
22a. NAME OF RESPONSIBLE INDIVIDUAL Anthony K. Amos		22b. TELEPHONE NUMBER (Include Area Code) 202/767-4935	22c. OFFICE SYMBOL AFOSR/NA													

## 19. ABSTRACT (Continued)

polyester rods 0.193 cm (0.076 in) in diameter and 18.72 cm (7.37 in) in length into machined 2024-T4 aluminum joints. Because a tetrahedral truss requires only two types of joints, the tetrahedrons and pyramids are constructed using the two types of joints. The cutting of the fiberglass rods, the machining of the aluminum joints and the final assembly of the tetrahedrons and pyramids are done with great care to minimize structural variability. *R*

The experimental results indicate that although the input waveform is a gated sinusoid, the output waveform has a complex shape. This may be due to internal reflections within the joints and the rods, as well as due to transmissions and reflections at the interfaces between the joints and the rods. Also, the amplitude of the output signal may be affected by the dissipation of the materials. Because the output waveform depends on the rods, joints and their interfaces, it may be useful in the nondestructive evaluation (NDE) of truss structures.

A significant observation obtained in this study is the experimental (qualitative) verification of reciprocity between input and output. For example, if the input is applied at joint 2 and the output is observed at joint 5 of a pyramid, the same output will be observed at joint 2 if the input is applied at joint 5 of the structure. More complex quantitative analyses are currently underway.

The results of this preliminary study demonstrate that experimental wave propagation studies can be successfully conducted on a truss model consisting of rods and joints. Thus, this study provides an experimental basis for wave propagation investigations in LSS.

## ACKNOWLEDGMENTS

The Air Force Office of Scientific Research (Project Monitor, Dr. Anthony K. Amos) is gratefully acknowledged for its support of this research.

Approved for public release;  
distribution unlimited.

AIR FORCE OFFICE OF SCIENTIFIC RESEARCH  
NOTICE OF RELEASE  
THIS  
COPY  
DATE  
REASON  
Chief, Test and Evaluation Division

# NOTICE

This document was prepared under the sponsorship of the Air Force. Neither the US Government nor any person acting on behalf of the US Government assumes any liability resulting from the use of the information contained in this document. This notice is intended to cover WEA as well.

Accession For	
NTIS CRA&I	<input checked="" type="checkbox"/>
DTIC TAB	<input type="checkbox"/>
Unannounced	<input type="checkbox"/>
Justification	
By	
Distribution	
Availability Codes	
Dist	Avail. or Spec.
A-1	



## TABLE OF CONTENTS

	<u>Page</u>
ABSTRACT . . . . .	1
ACKNOWLEDGMENTS . . . . .	3
NOTICE . . . . .	4
TABLE OF CONTENTS . . . . .	5
INTRODUCTION . . . . .	7
BACKGROUND . . . . .	7
SCOPE OF PRESENT WORK . . . . .	7
EXPERIMENTAL PROCEDURE . . . . .	9
MATERIAL . . . . .	9
EQUIPMENT . . . . .	9
PREPARATION AND CHARACTERIZATION OF THE RODS AND THE JOINTS . . . . .	9
CONSTRUCTION TECHNIQUES OF ELEMENTAL STRUCTURES . . .	10
TESTING USING ULTRASONICS . . . . .	11
RESULTS AND DISCUSSION . . . . .	15
RESULTS OF ULTRASONICS . . . . .	15
DISCUSSION . . . . .	17
CONCLUSIONS AND RECOMMENDATIONS . . . . .	20
REFERENCES . . . . .	22
TABLES . . . . .	23
FIGURES . . . . .	26
APPENDIX A	
METHODS FOR CUTTING THE FIBERGLASS REINFORCED COMPOSITE RODS, EQUIPMENT AND RESULTS . . . . .	46

## TABLE OF CONTENTS (CONT'D)

	<u>Page</u>
APPENDIX B	
ULTRASONIC TEST SYSTEM . . . . .	54
APPENDIX C	
DESIGN OF JOINTS FOR THE TETRAHEDRAL TRUSS . . . . .	57
APPENDIX D	
CHARACTERIZATION DATA OF JOINTS AND RODS USED IN THE STRUCTURES . . . . .	65
APPENDIX E	
ORIENTATION AND LABELLING OF THE BASIC STRUCTURES .	68

## INTRODUCTION

### BACKGROUND

Lattice trusses have been and are used to span large areas with only a few intermediate supports. These structures combine low cost with light weight to make them quite practical. In addition, because of their ease of packaging, transporting, and assembly in space, they are being strongly considered for use in large space structures (LSS) such as solar power stations, large mirrors, antennae, and power systems for supporting space operations. An important feature of many proposed LSS is that they have a basic pattern of configuration which is repeated many times.

Lattice trusses can be found in many applications on earth where low cost and low set up time are important. Many towers used for electricity, telephone communications, and oil wells rely on various lattice structures for their support. The vibration and wave propagation characteristics of these structures can affect their performance, integrity and the ability to non-destructively assess that integrity.

### SCOPE OF PRESENT WORK

In this preliminary study, the wave propagation characteristics of a tetrahedral truss model consisting of fiberglass reinforced composite rods and aluminum joints are observed experimentally. The fabrication of the truss model is done with great care to minimize structural variability.

Longitudinal ultrasonic transducers are coupled to the joints of the truss model. The input signal consists of a gated sinusoid having a center frequency of 280 kHz. The signal introduces a corresponding ultrasonic wave into the truss structure via a transmitting ultrasonic transducer. The wave is detected by a receiving ultrasonic transducer after it has propagated through the truss structure. Then an output signal is produced, corresponding to the detected wave.

The output waveforms for various locations of transmitting and receiving transducers on the truss model are obtained experimentally. This preliminary study provides an experimental basis for subsequent wave propagation investigations in truss structures.

## EXPERIMENTAL PROCEDURE

### MATERIAL

The material included Glastic HIR Fiberglass Reinforced Polyester Rods (Glastic part number 6033076) and joints machined from 2024-T4 Aluminum; Devcon five minute epoxy was used as the adhesive for the rods and the joints.

### EQUIPMENT

Refer to Appendix A for the rod cutting system and to Appendix B for the ultrasonic attenuation test system.

### PREPARATION AND CHARACTERIZATION OF THE RODS AND THE JOINTS

The rods with a measured diameter of  $0.193 \text{ cm} \pm 0.001$  ( $0.076 \text{ in.}$ ) were cut to  $18.69$  and  $18.74 \text{ cm}$  lengths ( $7.36 \text{ in}$  and  $7.376 \text{ in}$ , respectively). The need for two lengths of rods is due to the geometry of the joints and is explained further in Appendix C. Care was taken to ensure that minimal damage was caused to the cut ends and several methods were attempted until satisfactory results were obtained. The method used and the others that were tried are described in Appendix A along with an assessment of the effectiveness of each method. The lengths were cut to within  $\pm 0.005 \text{ cm}$  ( $0.002 \text{ in}$ ) and each rod was weighed. The ends of the rods were sealed with epoxy to prevent flaring and to fill possible cracks. Microscopic examination of the ends was conducted to ensure that no significant damage was done by the cutting.

Two types of joints were machined for this structure. Joint type A was characterized by the four holes drilled on the spherical surface which made 45 degree angles with the top center hole and were equally spaced apart. Type B joints had four of the holes on the spherical surface drilled to make 60 degree angles with the center hole and the angles of 70.5, 109.5, 70.5 and 109.5 degrees between each other when viewed from the top. The design and characterization of these joints is thoroughly explained in Appendix C.

After machining, the joints were separated by type and weight. The diameter and height of each joint was measured and the depth and orientation of the holes were examined for correctness. The characterization data of the joints and the rods used in the structures are contained in Appendix D.

#### CONSTRUCTION TECHNIQUES OF ELEMENTAL STRUCTURES

Two joints were glued to one rod for the purposes of the most elementary testing. The epoxy was placed in the central hole of each joint and then the rod was carefully inserted into the holes. Sufficient pressure to force excess epoxy from the hole was applied and then the excess was wiped off. Care had to be taken to prevent the end of the rod from getting frayed as it was inserted. To ensure that the rod was properly seated in the hole, an equal length rod was used for comparison. The rods were so close

fitting that joint-rod pressure along the rod axis had to be maintained on the parts to prevent the rods from being forced from the holes.

The tetrahedron is one of the basic structures of the tetrahedral truss and several of them were constructed for testing purposes. The gluing technique was the same as described for the single rod. The orientation of the joints has to be observed for proper construction. Two of each joint, types A and B, were necessary for this structure. Five rods of length 18.74 cm (7.376 in) and one 18.69 cm (7.36 in) rod were needed. To prevent residual stress from being imposed upon the rods, care was taken to ensure that there was no twist in them while the epoxy was drying.

The pyramid is also a basic structure of this truss. Three of them were constructed using many of the same techniques and principles mentioned above. For this structure it is best to put together the base and then to add two of the side rods to the base. Then glue the other two side rods to the top joint which can then be attached to the base. The last step is to glue the two side rods to the top joint. In this structure it is extremely important not to introduce any residual stresses which is easy to do if one is not careful.

#### TESTING USING ULTRASONICS

The ultrasonic attenuation test system described in Appendix B was used for this testing. The clamping of the

transducers to the joints was done by a modified hair clip. The set-up in Fig. B-2 shows a one-rod ultrasonic test assembly. A simple test was used to determine that the clamps provided consistent as well as adequate pressure to provide a proper signal output from the transducers. Although the "saturation pressure" defined by Williams, Nayeb-Hashemi, and Lee [1] may not have been used to provide for the maximum output, the pressure used was approximately consistent. The results obtained through these experiments with ultrasonic attenuation provide qualitative information which is useful, but are not rigorous enough to yield much quantitative information.

A thin layer of the couplant AET SC-6 was applied to the joint-transducer interface. The thickness of the couplant was maintained constant. This is very important because of the effect that its thickness has on the attenuation recorded as determined by Williams, Nayeb-Hashemi, and Lee [1]. The thickness was not measured for these experiments because they deal with qualitative assessments.

After application of the couplant, the transducer was clamped to the flat face of the joint to be tested. It was found that it made no significant difference to the results by the means of support for the structures. The specimens were set on a flat surface with the wires freely hanging.

Williams, Nayeb-Hashemi, and Lee [1] found that the

ultrasonic attenuation in graphite fiber composites varied with the input frequency. Taking this into consideration, a wider range of frequencies (.1 to 4 MHz) was tested to determine the best range. A frequency of about 280 kHz was used in these experiments and the natural frequency of the transducers lies in the vicinity of 300 kHz.

The first set of tests was conducted on the specimens with two joints glued to one rod. (See Fig. B-2) Initially, the transmission was input from one joint and received at the other, and then vice versa. In these experiments, the direction of the signal was changed by the switching of the two leads. It was judged that it would yield non-useful results to have also switched around the transducers each time. The reason is that the couplant thickness would have been changed which would have affected the results. These tests were directed towards order of magnitude attenuation characteristics and concerned with detecting any interesting behavior exhibited by symmetrical or similar configurations. They were conducted to yield some information of the consistency with which the rods and joints were glued together. Throughout the experiments the transducers were not differentiated and assumed to yield similar results.

The testing of the tetrahedrons was systematic to encompass all possible characteristic transmissions with no unnecessary overlap. Appendix E shows how the tetrahedron was labelled according to the joints. (See Fig. E-3) The testing proceeded from joint 1 to 2, then 1 to 3, and then

1 to 4. Next, it went from joint 2 to 3, 2 to 4, and then from 3 to 4, which completed the characterization because the reverse tests (i.e. 4-1, 3-1, 2-1, etc.) were conducted while the appropriate transducer connections were made. To characterize the transmission between any two joints, a photograph was taken of the input and output signals.

Testing of the pyramids was conducted in a very similar manner as the tetrahedrons. Since the pyramid has five joints, the number of combinations was larger but this caused no problem. Each set of joints was again characterized by a photograph of the input and output which appeared on the oscilloscope. The characteristic number of photographs for the pyramids was 10 because of its geometry. Two pyramids were randomly chosen for these characterization experiments. The testing proceeded in the following sequence of nodal pairs: 1-2, 2-1, 1-3, 3-1, 1-4, 4-1, 1-5, 5-1, 2-3, 3-2, 2-4, 4-2, 2-5, 5-2, 3-4, 4-3, 3-5, 5-3, 4-5, and 5-4.

## RESULTS AND DISCUSSION

### RESULTS OF ULTRASONICS

The results of all these tests are in Figs. 3 through 20.

The rods joined to two joints were tested and the following observations were made. Reversing the input and output usually varied the output amplitude slightly but the waveforms were quite similar. A gradual decay of the output signal was observable.

In Tables 1 and 2, the interpretation of the data for the tetrahedrons is given. The input joint is specified along the left column and the output joint is given along the top row. The symbols above the main diagonal specify the relationships, if any, of the outputs. Those below the diagonal describe the reciprocal nature found in the structures. The definitions of the notation are given below each table. To elaborate, for the combination 2-1, the notation C12 means that the output of 2-1 is essentially equivalent to the output of 1-2. The notation D happens to be applicable to both tests but the C13's, C23's, C14's, C24's, and C34's are distinct and don't indicate similar waveforms between the tables unless otherwise stated.

Symmetry occurs across the main diagonal. The B1 means that these outputs are very similar to one another and this also applies in Tables 2 and 3 to B2 through B6.

The results of tetrahedron II are analogous to tetra-

hedron I in many ways even though the waveforms are different. Tetrahedron II also exhibits the reciprocity across the main diagonal. An interesting characteristic is the strong similarity between the outputs of 1-3, 1-4, 2-3, and 2-4 which exhibit geometric symmetry (See Figs. 8, 9, and 10). In a qualitative sense, this could indicate that tetrahedron II was more uniformly constructed than tetrahedron I, which doesn't show as much symmetry. It is also noted that the waveforms of tetrahedron I and II from joints 1-2 are comparable to the output of a single rod test assembly.

The results of the ultrasonic attenuation tests for the pyramids are summarized in Table 3. The outputs from the combinations 1-2, 1-3, 1-4 and 1-5 from both pyramids fall into a group with basic similarity and they also are geometrically similar (See Figs. 11 and 12, and Figs. 16 and 17). These structures also demonstrate the reciprocal nature of its nodal combinations, as in the tetrahedron structures.

The remaining six different nodal combinations form three interesting pairs. Combinations 2-3, and 4-5, 2-4 and 3-5, and 2-5 and 3-4 form very similar pairs. Specifically, Figs. 13, 18, 19 and 20 display much similarity. Referring to Fig. E-6, the geometric similarity of the pairs mentioned can be observed.

It is important to observe that although the joints and the adhesive bonds may vary between the pyramids, they did produce surprisingly similar waveforms.

## DISCUSSION

The complex shape of the output waveform is thought to be caused by the geometry of the joints as well as the nature of the rod-joint interface. The signal is transmitted through the joint and into the rod through the rod-joint interface. At this point, transmission and some reflection are likely to occur. The reflection is then reflected from the joint-transducer interface to start the cycle again but with less amplitude than the original input. The phase lag between the initial transmission and the subsequent reflections may cause the complex output through superposition. In addition, the slight variations in the geometry of the joints and the rod-joint interfaces may have been a cause of variations in the outputs. Even so, the output waveforms exhibit macroscopic similarity of many types. The results of this testing have yielded useful information on the phenomena of the structures.

The single rod specimens like all other joint combinations produced essentially the same waveform regardless of which joint was used for the input and which for the output. Since it was suggested that the complex waveforms were a result of joint geometry and rod-joint interface, it makes sense that the nodal pairs would exhibit reciprocity. The joints were made with extreme care. Likewise, the bonding between the rods and the joints was done as consistently

as possible, as well as the cutting of the rods. These variables could be considered fixed within a certain tolerance. The results show that though no two nodal pairs replicate each other's response, an overall similarity can be found in certain cases which agrees with what could be expected from geometric considerations.

It was mentioned that tetrahedron II may have been more uniformly constructed than tetrahedron I. Tetrahedron I exhibited similarity in the 1-3 and 1-4 as well as in the 2-3 and 2-4 transmissions. Tetrahedron II showed similarity in all of the transmission combinations which are geometrically alike. These results tend to indicate that tetrahedron II was probably more uniformly constructed than tetrahedron I, but the extent to which this is true cannot be stated quantitatively here.

The output from joints 1-2 is roughly similar to a rod with only two joints. (Refer to Fig. E-3 for the convention used for labelling.) This would seem to be the case because the transmission path for this joint combination is most similar to the single rod/two joint combination.

The pyramids are good examples of structures with much geometric symmetry. The results from these specimens were quite well defined and obeyed the geometric symmetry. The transmissions from joint 1 to joints 2, 3, 4, and 5 were very similar. The very similar combinations were 2-3 and 4-5, 2-4 and 3-5, and 2-5 and 3-4.

The output from the two pyramids, even with all their physical differences showed a definite correspondence with each other. This possibly could mean that on the macroscopic level, the symmetry of the structure begins to dominate over the smaller incongruities.

## CONCLUSIONS AND RECOMMENDATIONS

In this preliminary study, the wave propagation characteristics of a tetrahedral truss model consisting of fiberglass reinforced composite rods and aluminum joints are observed experimentally. The truss consists of fiberglass reinforced polyester rods 0.193 cm (0.076 in) in diameter and 18.72 cm (7.37 in) in length inserted into machined 2024-T4 aluminum joints. The fabrication of the truss structure is done with great care to minimize structural variability.

Longitudinal ultrasonic transducers are coupled to the joints of the truss models. The input signal consists of a gated sinusoid having a center frequency of 280 kHz. Because a tetrahedral truss can be constructed from basic repeating units of tetrahedrons and pyramids, only tetrahedrons and pyramids are considered. Also, because a tetrahedral truss requires only two types of joints, the tetrahedrons and pyramids are constructed using the two types of joints.

Based on the results of this preliminary experimental study, the following conclusions can be made:

- (1) Although the input waveform is a gated sinusoid, the output waveform has complex shape. This may be due to internal reflections within the joints and the rods, as well as due to transmissions and reflections at the interfaces between the joints and the rods. Also the amplitude of the output signal may be affected by the dissipation of the materials.

- (2) Experimental (qualitative) verification of reciprocity between input and output for wave propagation in truss structures has been obtained. For example, if the input is applied at joint  $i$  and the output is observed at joint  $j$  of a truss, the same output will be observed at joint  $i$  if the input is applied instead at joint  $j$  of the structure.

Based on the results of this preliminary experimental study, the following recommendations can be made:

- (1) Because the details of the output waveform depend on the rods, joints and their interfaces, ultrasonics may be useful in the nondestructive evaluation (NDE) of truss structures. Truss models with and without intentional defects in the rods, joints and/or their interfaces should be fabricated and tested for wave propagation characteristics.
- (2) In this study, because a tetrahedral truss can be constructed from basic repeating units of tetrahedrons and pyramids, only tetrahedrons and pyramids are considered. Future studies in experimental wave propagation should consider a truss consisting of multiple repeating units. A simple truss to consider may be a planar truss with multiple bays [2,3].
- (3) There is little theoretical analysis of wave propagation in LSS [4]. Analytical bases should be developed to provide for the interpretation and the eventual prediction of wave propagation behavior in lattice structures.

## REFERENCES

- [1] J.H. Williams, Jr., H. Nayeb-Hashemi, and S.S. Lee, "Ultrasonic Attenuation and Velocity in AS/3501-6 Graphite Fiber Composite", Journal of Nondestructive Evaluation, Vol. 1, No. 2, June 1980, pp. 137-147.
- [2] J.H. Williams, Jr., R.H. Lailier, Jr., and S.S. Lee, "Wave Propagation Through "T" and "L" Lattice Joints", AFOSR Technical Report, October 1984.
- [3] J.H. Williams, Jr., R.A. Schroeder and S.S. Lee, "Dynamic Analyses of Two Dimensional Lattices", AFOSR Technical Report, August 1984.
- [4] A.K. Noor, "Assessment of Current State of the Art in Modeling Techniques and Analysis Methods for Large Space Structures", Modeling, Analysis, and Optimization Issues for Large Space Structures, NASA Conference Publication 2258, Proceedings of a Workshop held in Williamsburg, VA, May 13-14, 1982, National Aeronautics and Space Administration, Washington, D.C., 1983, pp. 5-32.

TABLE 1  
Results of Testing Tetrahedron I

Output Input	1	2	3	4
1	-	D	B1	B1
2	C12	-	B2	B2
3	C13	C23	-	E
4	C14	C24	C34	-

Notation:

Group

A - the output is roughly similar to other(s) of this type.

B(X) - the output is very similar to other(s) of this type.

C(X,Y) - the output is essentially equivalent to the  
combination (X,Y) specified.

D - the output is comparable to that of a single rod  
test assembly.

E - the output is not similar to other outputs.

TABLE 2

## Results of Testing Tetrahedral II

Output Input	1	2	3	4
1	-	D	B3	B3
2	C12	-	B3	B3
3	C13	C23	-	E
4	C14	C24	C34	-

## Notation:

## Group

A- the output is roughly similar to other(s) of this type.

B(X) - the output is very similar to other(s) of this type.

C(X,Y) - the output is essentially equivalent to the  
combination specified, (X,Y).

D - the output is comparable to that of a single rod  
test assembly.

E - the output is not similar to other outputs.

TABLE 3

## Results of Testing Pyramids I and II

Output Input	1	2	3	4	5
1	-	A	A	A	A
2	C12	-	B4	B5	B6
3	C13	C23	-	B6	B5
4	C14	C24	C34	-	B4
5	C15	C25	C35	C45	-

## Notation:

## Group

A - the output is roughly similar to the other(s) of this type.

B(X) - the output is very similar to other(s) of this type

C(X,Y) - the output is essentially equivalent to the combination (X,Y) specified.

D - the output is comparable to that of a single rod test assembly.

E - the output is not similar to other outputs.

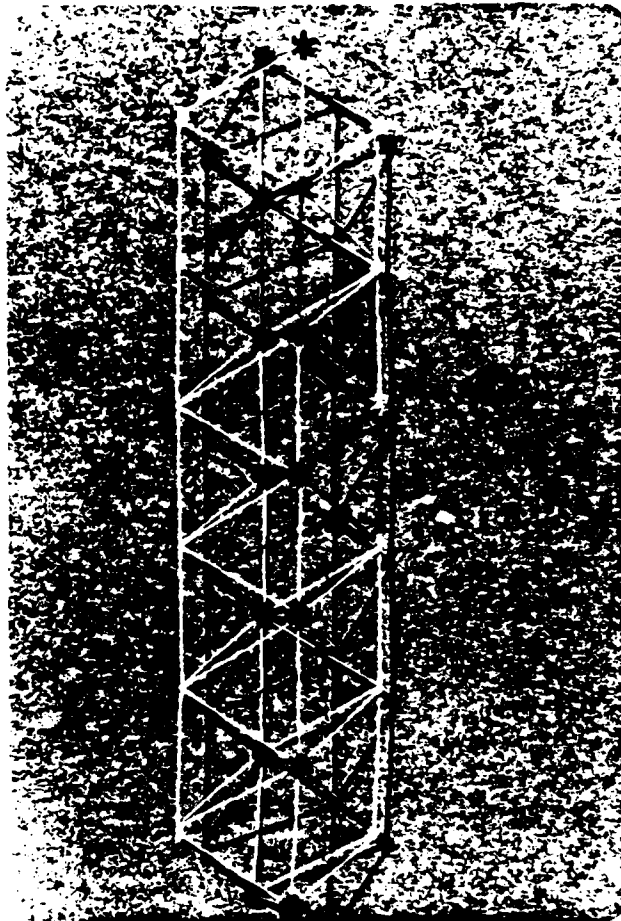


Fig. 1 Tetrahedral truss with fundamental structure identified.

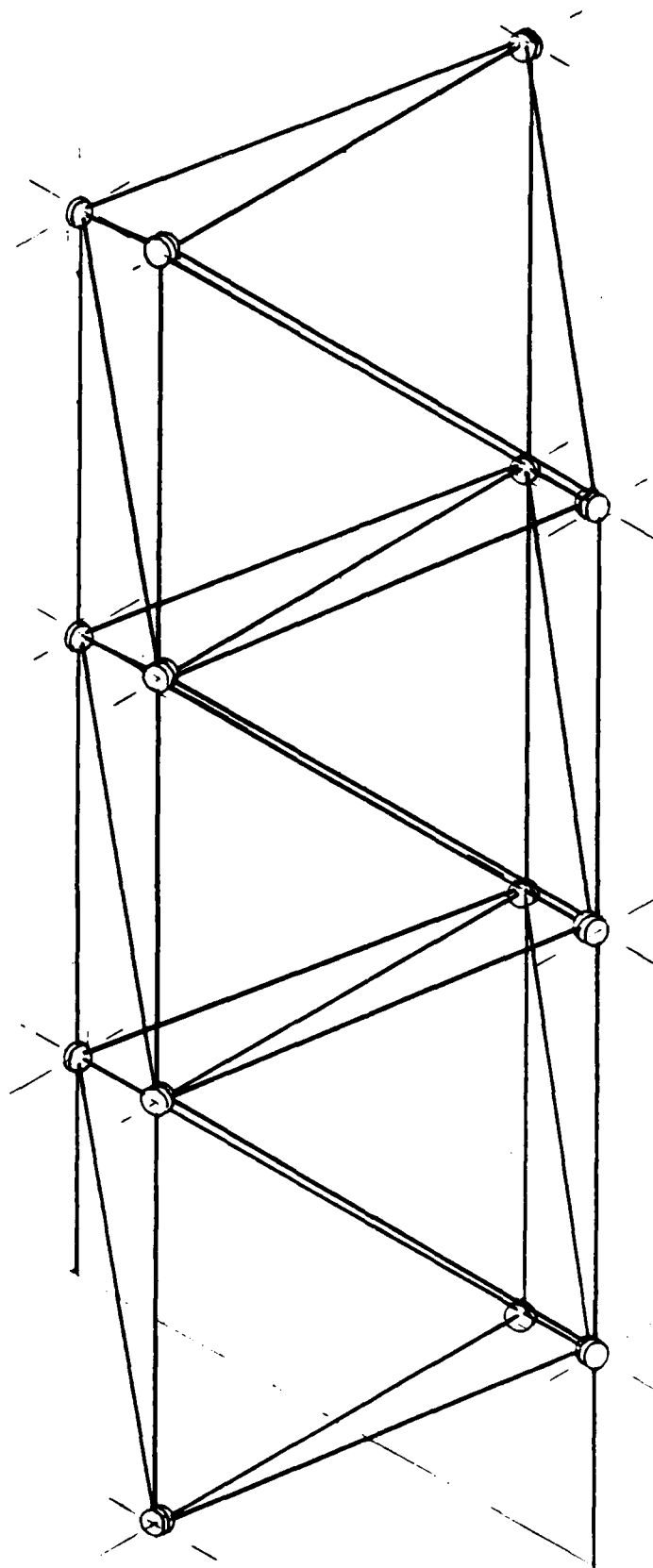
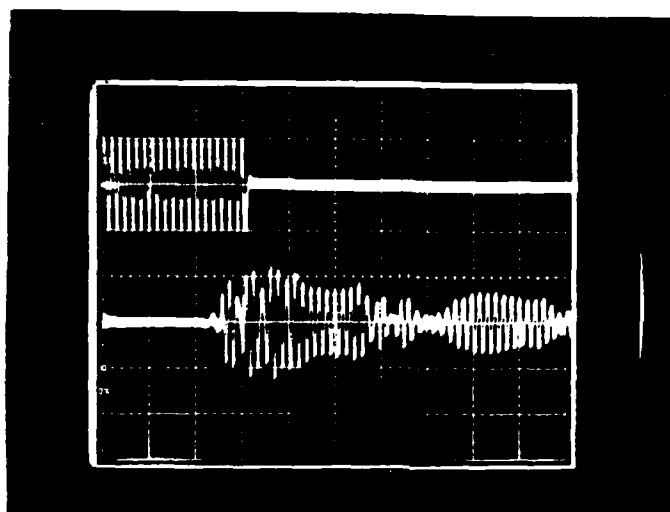


Fig. 2 Sketch of a tetrahedral truss.

INPUT: 100 Volts at 280 kHz.

INPUT

OUTPUT



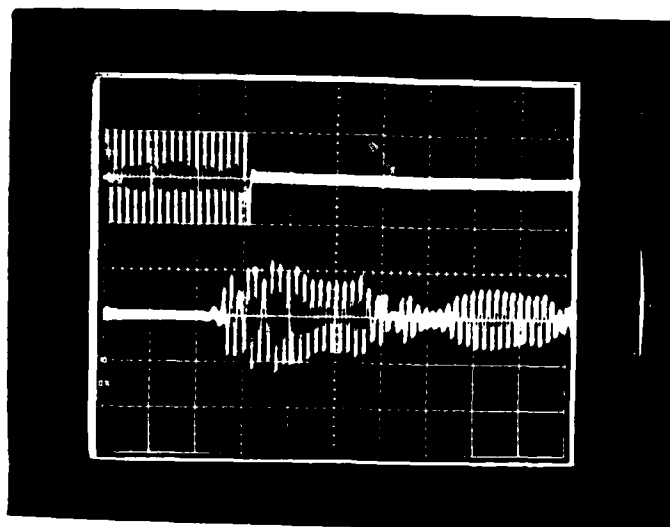
SWEEP  
.02 msec/div.

OUTPUT SCALE  
200 mvolt/div.

Pyramid III (2-5)

INPUT

OUTPUT



SWEEP  
.02 msec/div.

OUTPUT SCALE  
200 mvolt/div.

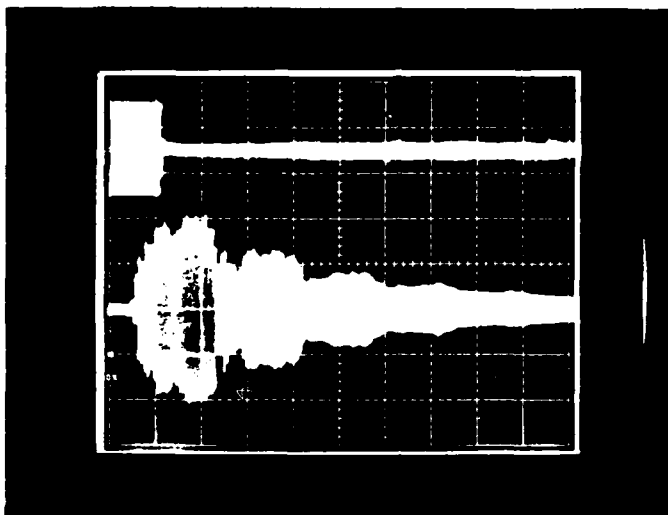
Pyramid III (5-2)

Fig. 3 Results

INPUT: 100 Volts at 280 kHz.

INPUT

OUTPUT



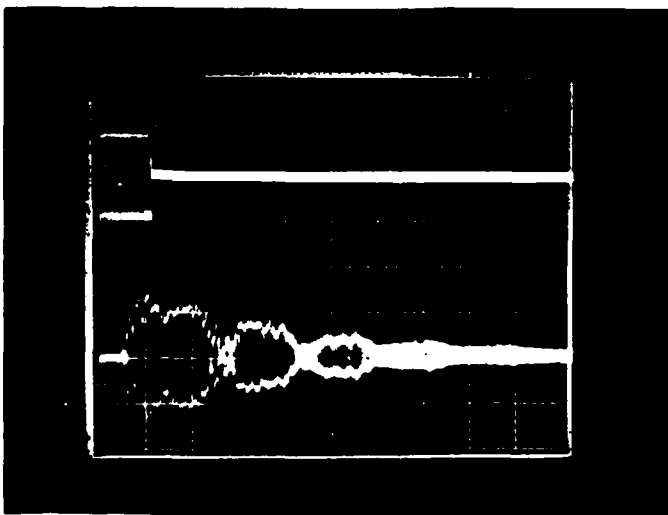
SWEEP  
.05 msec/div.

OUTPUT SCALE  
200 mvolts/div.

Single Rod- Specimen #1

INPUT

OUTPUT



SWEEP  
.05 msec/div.

OUTPUT SCALE  
200 mvolt/div.

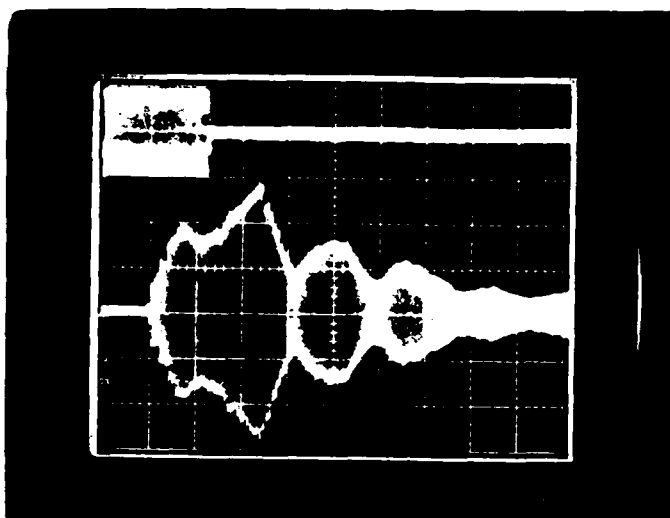
Single Rod- Specimen #1

Fig. 4 Results

INPUT: 100 Volts at 280 kHz.

INPUT

OUTPUT



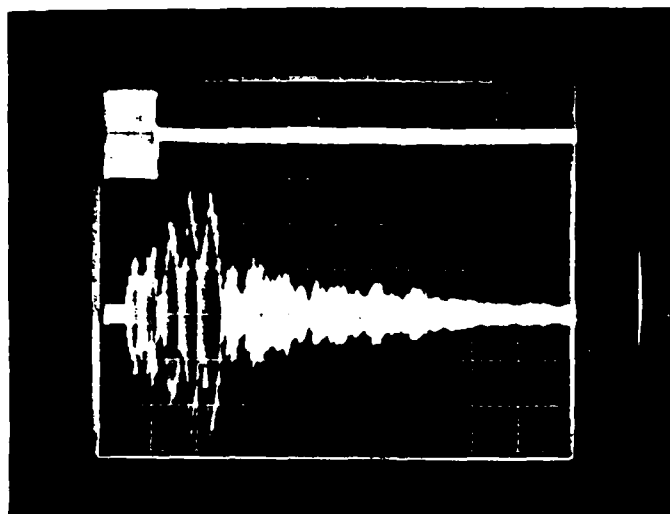
Tetrahedron I (2-1)

SWEEP  
.05 msec/div.

OUTPUT SCALE  
200 mvolt/div.

INPUT

OUTPUT



Tetrahedron I (3-1)

SWEEP  
.1 msec/div.

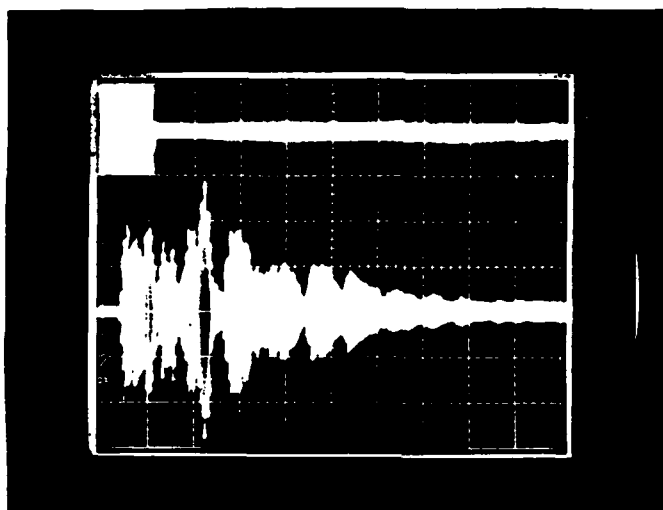
OUTPUT SCALE  
20 mvolt/div.

Fig. 5 Results

INPUT: 100 Volts at 280 kHz.

INPUT

OUTPUT



Tetrahedron I (4-1)

SWEEP

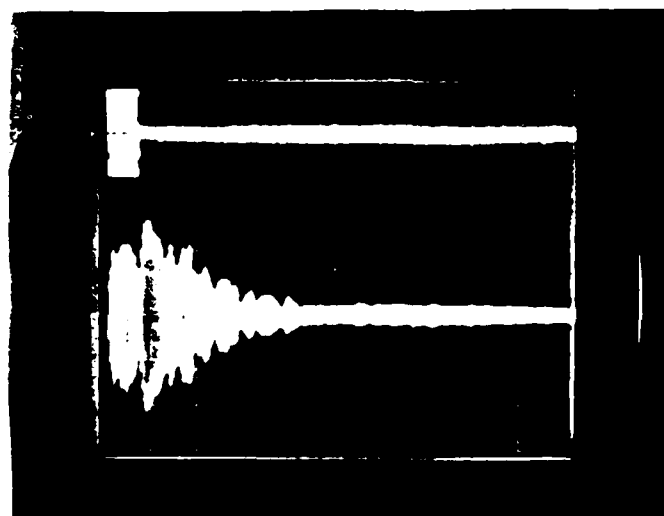
.1 msec/div.

OUTPUT SCALE

20 mvolt/div.

INPUT

OUTPUT



Tetrahedron I (2-3)

SWEEP

.1 msec/div.

OUTPUT SCALE

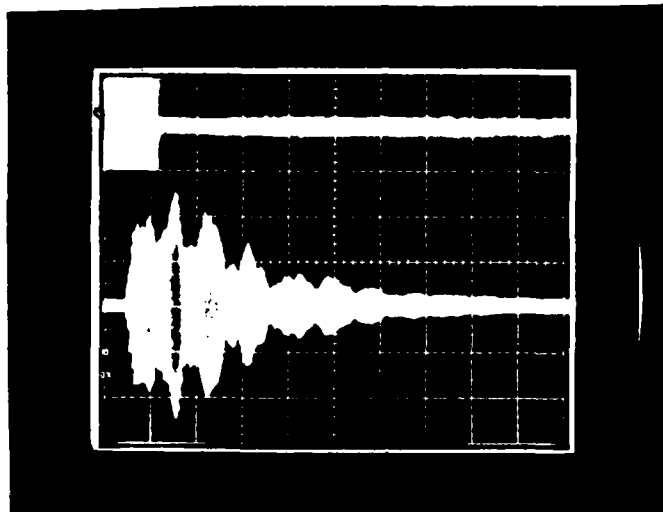
20 mvolt/div.

Fig. 6 Results

INPUT: 100 Volts at 280 kHz

INPUT

OUTPUT



Tetrahedron I (4-2)

SWEEP

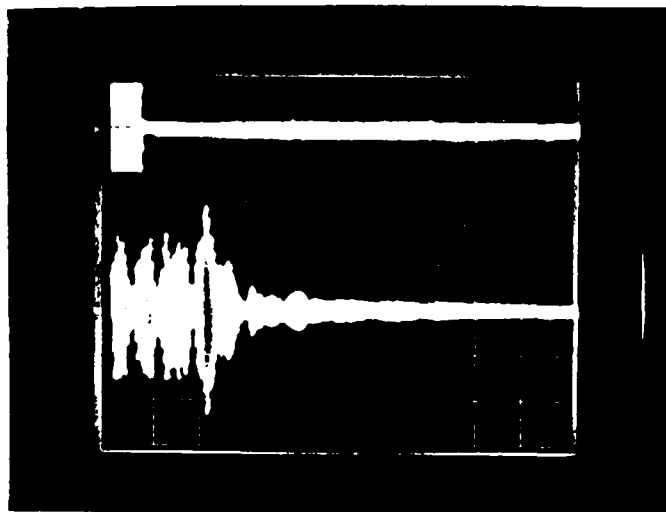
.1 msec/div.

OUTPUT SCALE

20 mvolts/div.

INPUT

OUTPUT



Tetrahedron I (4-3)

SWEEP

.1 msec/div.

OUTPUT SCALE

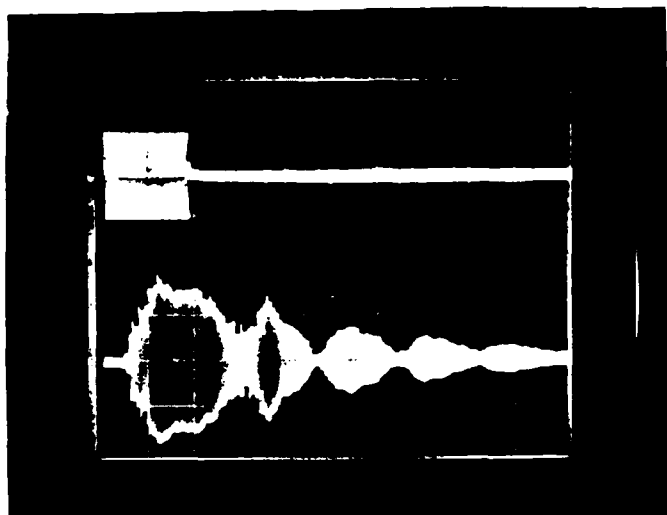
50 mvolt/div.

Fig. 7 Results

INPUT: 100 Volts at 280 kHz

INPUT

OUTPUT



Tetrahedron II (2-1)

SWEEP

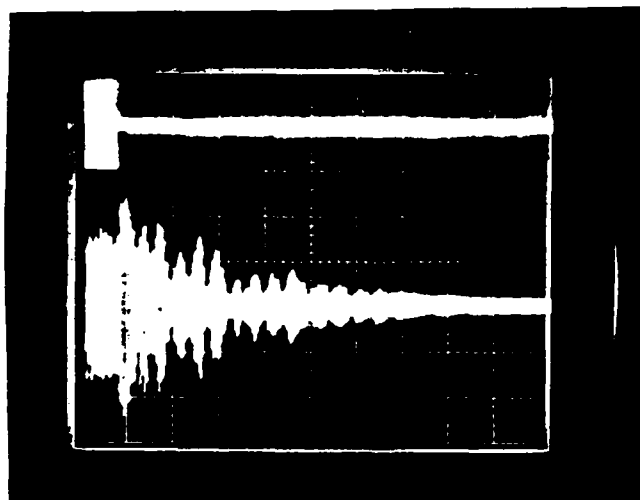
.05 msec/div.

OUTPUT SCALE

200 mvolt/div.

INPUT

OUTPUT



Tetrahedron II (3-1)

SWEEP

.1 msec/div.

OUTPUT SCALE

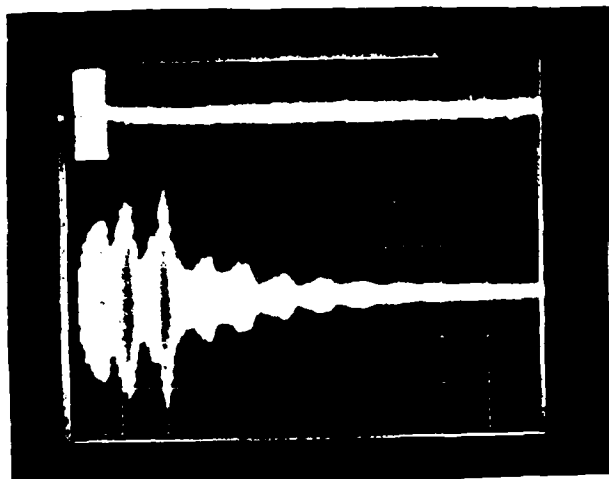
20 mvolt/div.

Fig. 8 Results

INPUT: 100 Volts at 280 kHz

INPUT

OUTPUT



Tetrahedron II (4-1)

SWEEP

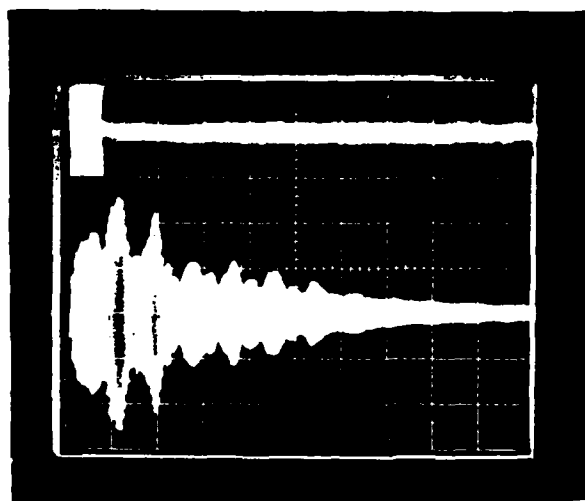
.1 msec/div.

OUTPUT SCALE

50 mvolts/div.

INPUT

OUTPUT



Tetrahedron II (2-3)

SWEEP

.1 msec/div.

OUTPUT SCALE

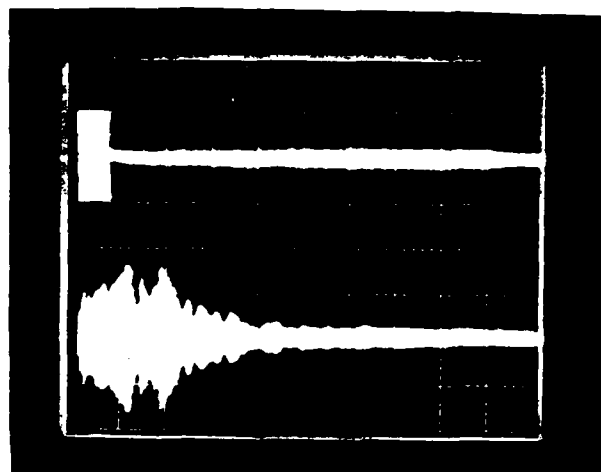
50 mvolts/div.

Fig. 9 Results

INPUT: 100 Volts at 280 kHz

INPUT

OUTPUT



SWEEP

.1 msec/div.

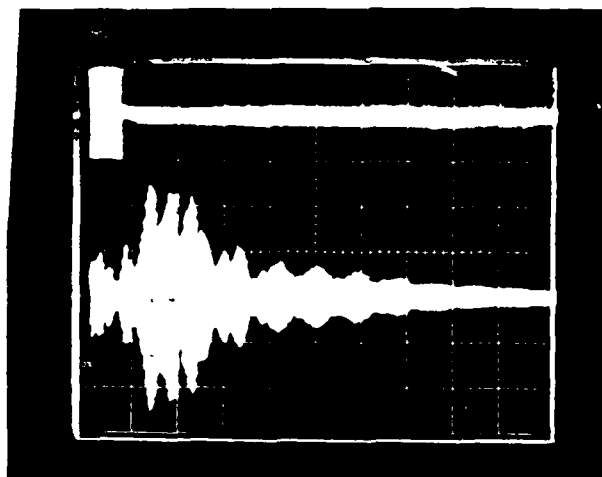
OUTPUT SCALE

50 mvolt/div.

Tetrahedron II (4-2)

INPUT

OUTPUT



SWEEP

.1 msec/div.

OUTPUT SCALE

50 mvolts/div.

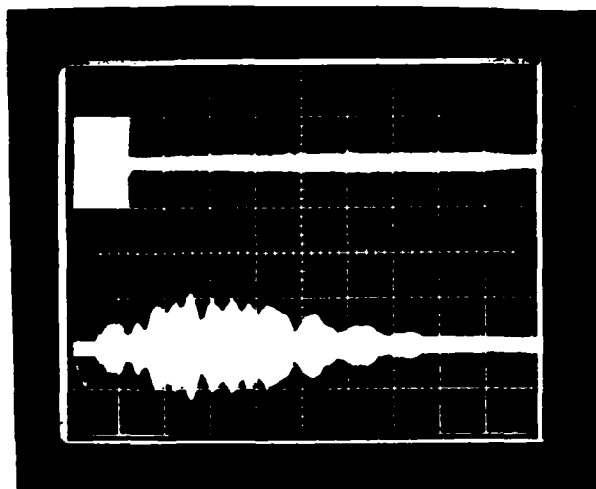
Tetrahedron II (3-4)

Fig. 10 Results

INPUT: 100 Volts at 280 kHz

INPUT

OUTPUT



SWEEP

.1 msec/div.

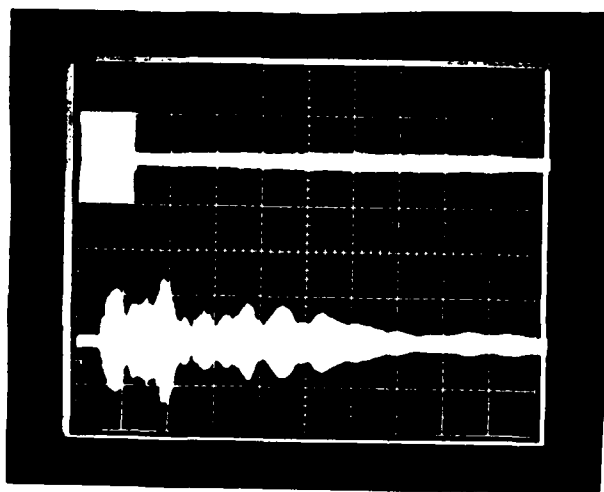
OUTPUT SCALE

50 mvolts/div.

Pyramid I (1-2)

INPUT

OUTPUT



SWEEP

.1msec/div.

OUTPUT SCALE

50 mvolts/div.

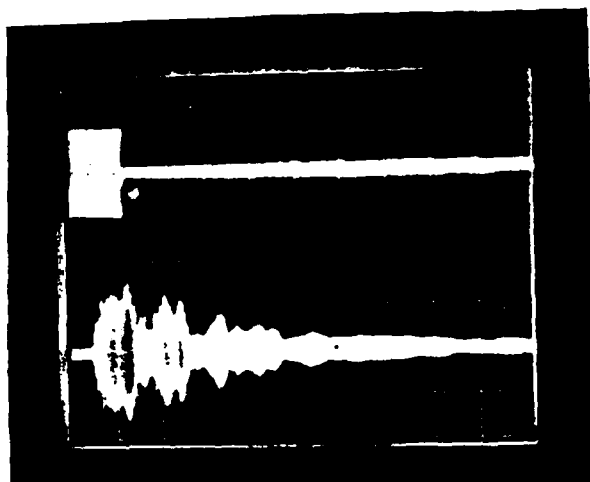
Pyramid I (1-3)

Fig. 11 Results

INPUT: 100 Volts at 280 kHz

INPUT

OUTPUT



Pyramid I (1-4)

SWEEP

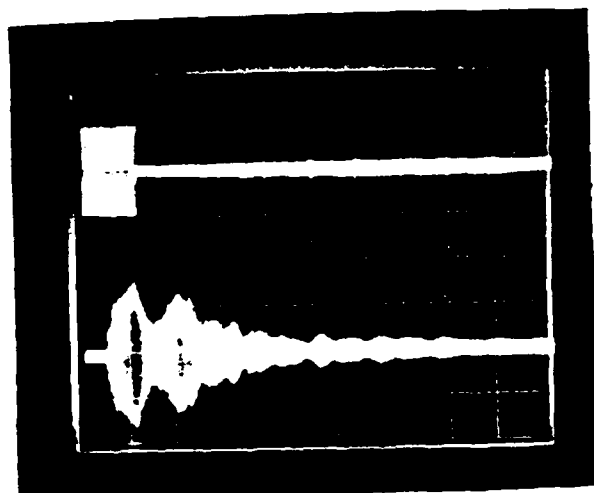
.1 msec/div.

OUTPUT SCALE

50 mvolts/div.

INPUT

OUTPUT



Pyramid I (1-5)

SWEEP

.1 msec/div.

OUTPUT SCALE

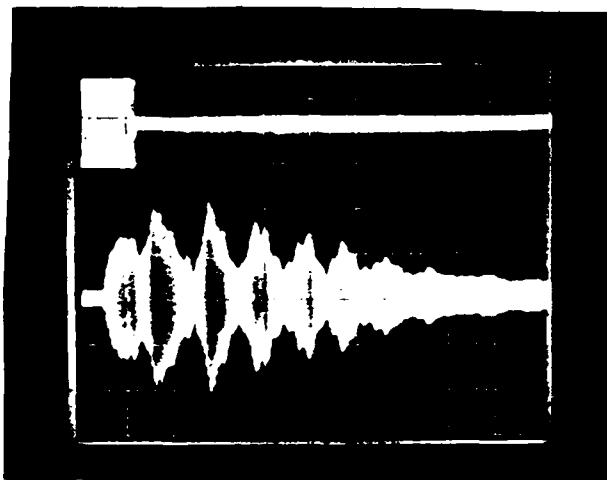
50 mvolts/div.

Fig. 12 Results

INPUT: 100 volts at 280 kHz

INPUT

OUTPUT



SWEEP

.1msec/div.

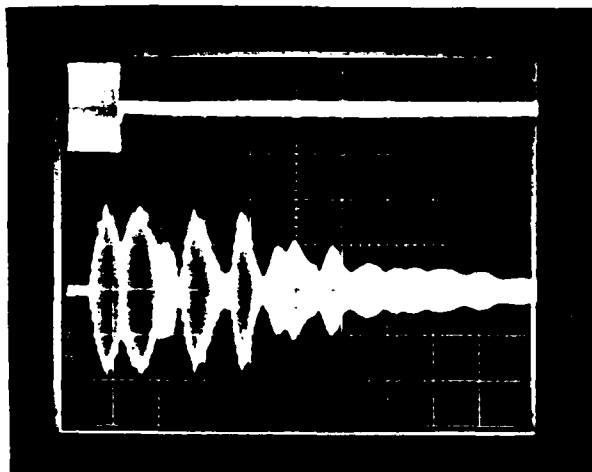
OUTPUT SCALE

50 mvolts/div.

Pyramid I (3-2)

INPUT

OUTPUT



SWEEP

.1 msec/div.

OUTPUT SCALE

50 mvolts/div.

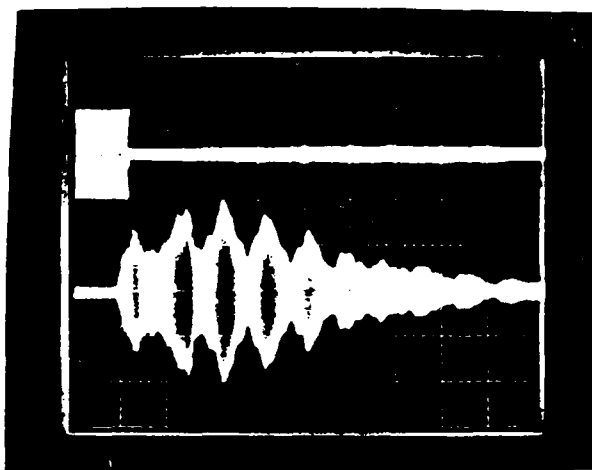
Pyramid I (4-5)

Fig. 13 Results

INPUT: 100 Volts at 280 kHz

INPUT

OUTPUT



SWEEP

.1 msec/div.

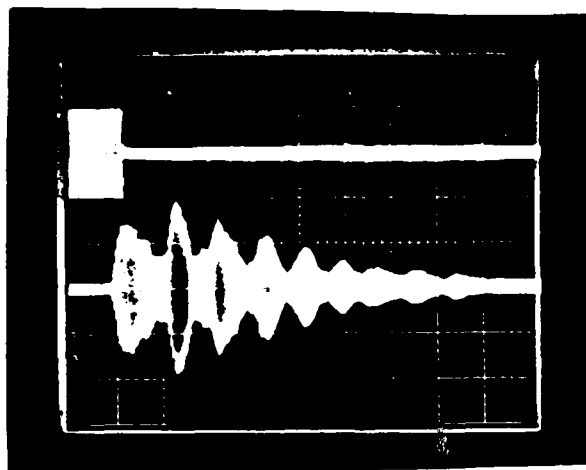
OUTPUT SCALE

50 mvolts/div.

Pyramid I (4-2)

INPUT

OUTPUT



SWEEP

.1 msec/div.

OUTPUT SCALE

50 mvolts/div.

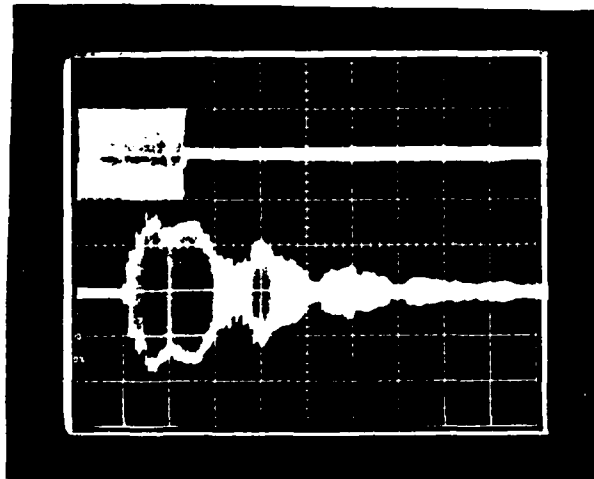
Pyramid I (5-3)

Fig. 14 Results

INPUT: 100 Volts at 280 kHz

INPUT

OUTPUT



SWEEP

.05 msec/div.

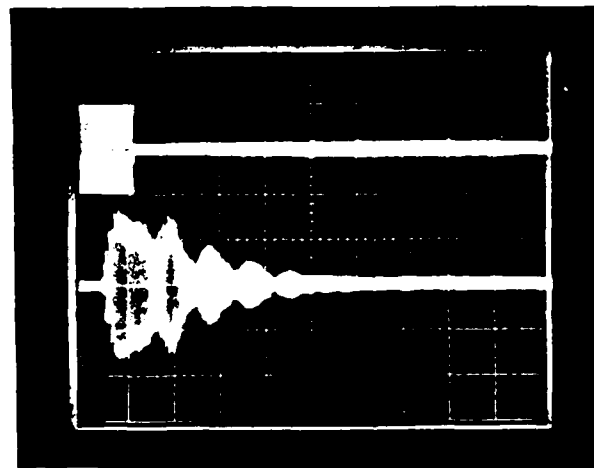
OUTPUT SCALE

200 mvolts/div.

Pyramid I (5-2)

INPUT

OUTPUT



SWEEP

.1 msec/div.

OUTPUT SCALE

200 mvolts/div.

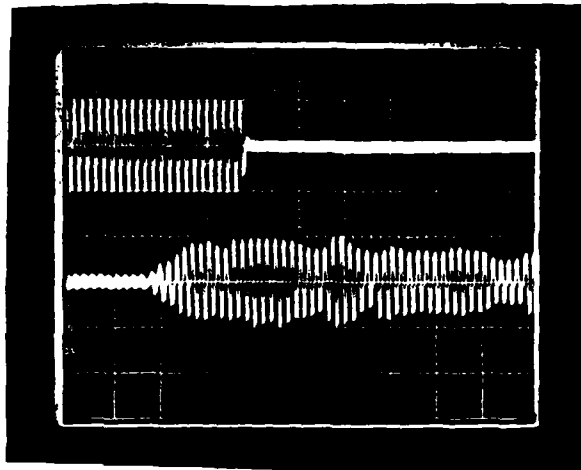
Pyramid I (4-3)

Fig. 15 Results

INPUT: 100 Volts at 280 kHz

INPUT

OUTPUT



SWEEP

.02 msec/div.

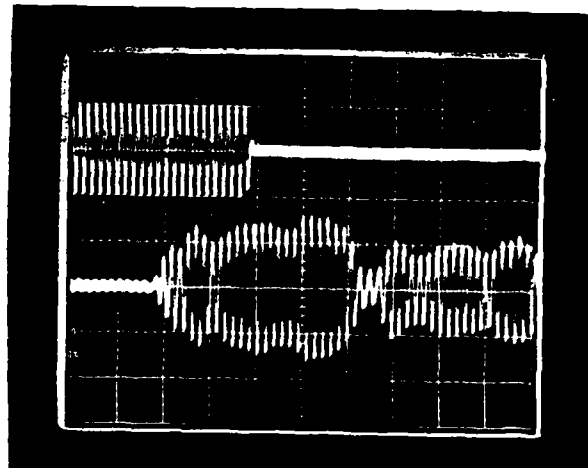
OUTPUT SCALE

50 mvolts/div.

Pyramid II (1-2)

INPUT

OUTPUT



SWEEP

.02 msec/div.

OUTPUT SCALE

50 mvolts/div.

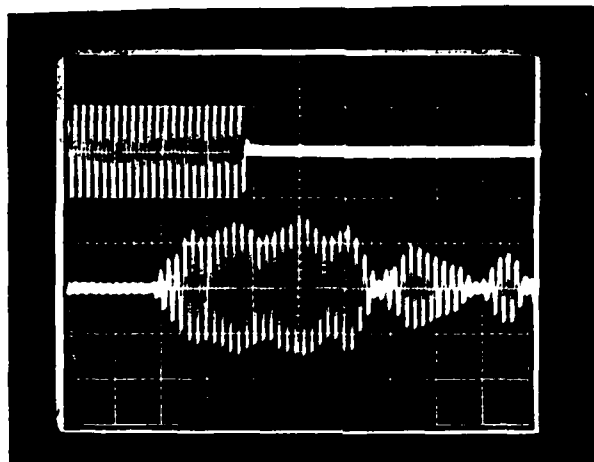
Pyramid II (1-3)

Fig. 16 Results

INPUT: 100 Volts at 280 kHz

INPUT

OUTPUT



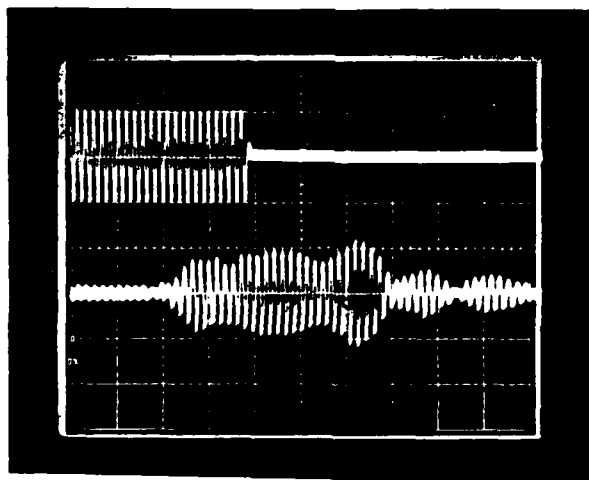
SWEEP  
.02 msec/div.

OUTPUT SCALE  
50 mvolts/div.

Pyramid II (1-4)

INPUT

OUTPUT



SWEEP  
.02 msec/div.

OUTPUT SCALE  
50 mvolts/div.

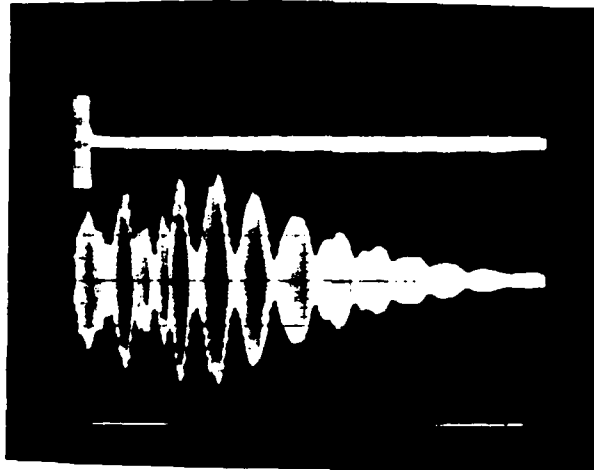
Pyramid II (1-5)

Fig. 17 Results

INPUT: 100 Volts at 280 kHz

INPUT

OUTPUT



SWEEP

.1 msec/div.

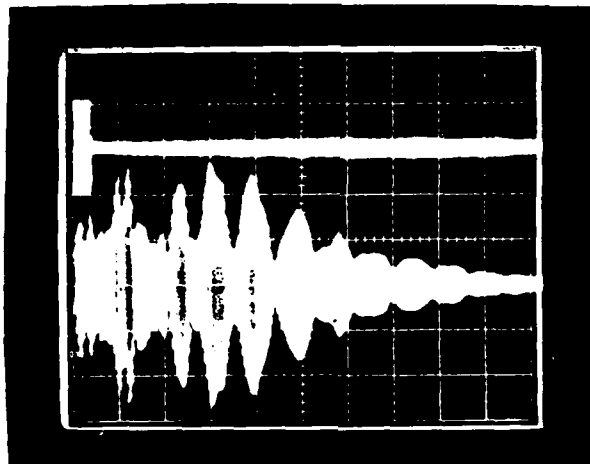
OUTPUT SCALE

50 mvolts/div.

Pyramid II (2-3)

INPUT

OUTPUT



SWEEP

.1 msec/div.

OUTPUT SCALE

50 mvolts/ div.

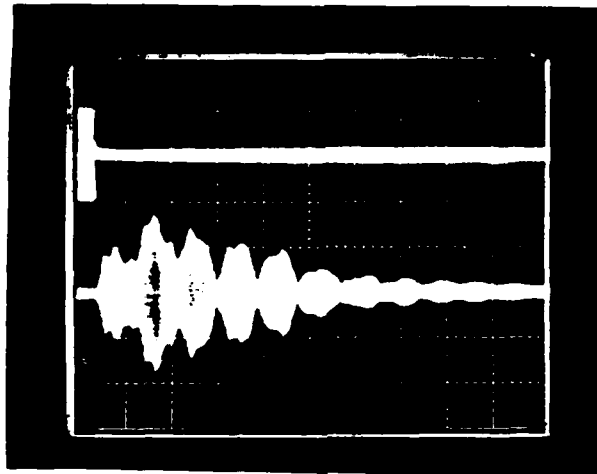
Pyramid II (4-5)

Fig. 18 Results

INPUT: 100 Volts at 280 kHz

INPUT

OUTPUT



SWEEP

.1 msec/div.

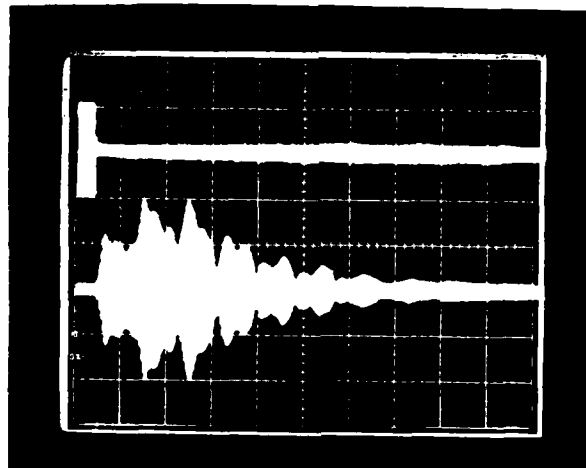
OUTPUT SCALE

50 mvolts/div.

Pyramid II (2-4)

INPUT

OUTPUT



SWEEP

.1 msec/div.

OUTPUT SCALE

50 mvolts/div.

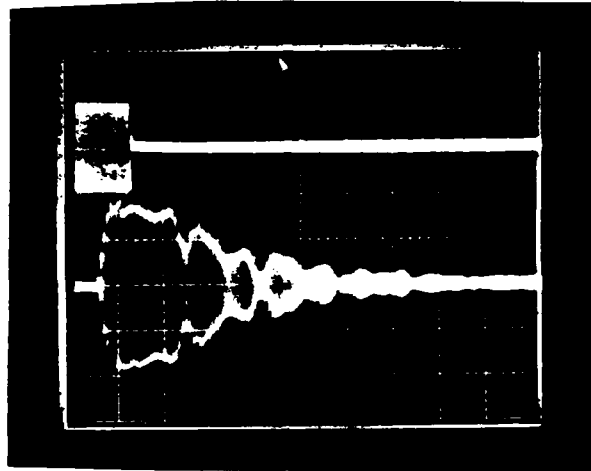
Pyramid II (3-5)

Fig. 19 Results

INPUT: 100 Volts at 280 kHz

INPUT

OUTPUT



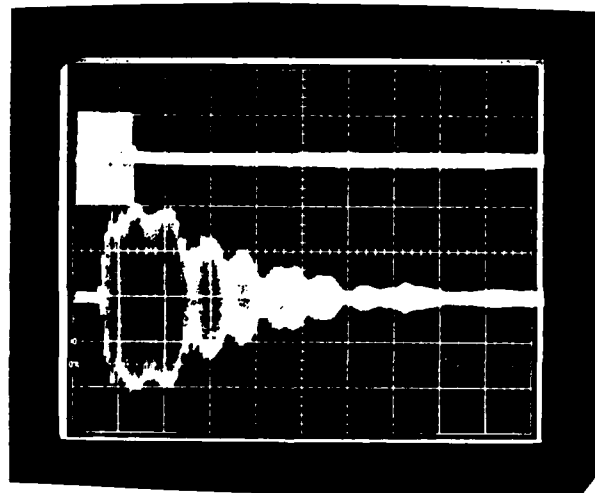
SWEEP  
.05 msec/div.

OUTPUT SCALE  
200 mvolts/div.

Pyramid II (2-5)

INPUT

OUTPUT



SWEEP  
.05 msec/div.

OUTPUT SCALE  
200 mvolts/div.

Pyramid II (3-4)

Fig. 20 Results

## APPENDIX A

### METHODS FOR CUTTING THE FIBERGLASS REINFORCED COMPOSITE RODS, EQUIPMENT AND RESULTS

#### Encasement in a hard setting wax

The rod was placed on a flat block of chaulk which was heated on a hotplate. The temperature of the chaulk block was raised above 90°F (which was the melting temperature of the wax). The wax was melted on the plate and made to cover approximately a one inch length of the rod. Care was taken to coat the entire circumference of the rod immersed in the wax. As it cooled, the wax formed a slight mound over the rod and secured it firmly to the chaulk block. The block was placed in a clamp fixture attached to the saw base and a diamond saw was used to cut through the wax, the fiber rod and a slight part of the block. The rate of cutting was mechanistically set at a slow speed and water was applied to provide cooling and lubrication. After cutting, the chaulk plate was again heated until the wax was melted and the fiber rods could be removed from it. Acetone was used to clean the remaining layer of wax from the rods. The wax was carefully wiped off with soft paper towels. (Tests were conducted earlier to see if the rod was dissolved or affected by the acetone. There were no apparent effects.)

To the naked eye, the rods cut by this method looked as though there was little or no flaring of the rod ends.

Further examination under a microscope confirmed that there was extremely little flaring and it appeared that the rod encasement and the matrix were undisturbed. (See Fig. A-1 and A-2) With the magnification and resolution available (50X), the possibility of microscopic cracking and damage to the resin could not be ruled out.

#### Simply supported end cutting

For this method, the fiber rod was pressed downward against a flat plate. The end of this plate was placed close to where the saw blade descended but just clear so that it was not cut. (See Fig. A-3.) Below this plate was the saw base which anchored the entire assembly. The rod was cantilevered and clamped to the upper plate about one inch from where the cut was made. The cut was made very close to the edge of the support plate and water was applied for cooling. The rate of cutting was approximately 0.06 cm/sec (0.025 in/sec).

With this method, several problems arose and were noted. One major problem was that the sawing damaged the rod ends significantly and caused flaring. In addition, a slight burning of the fiber was detectable where the saw finished the cut. The end was observed to be uneven because the fibers shifted as they were cut. These effects were noticable by eye so further examinations were not pursued.

Method Used - Mechanical clamping of the rod between aluminum plates

A fixture was machined to clamp and support the entire circumference of the rod during cutting to minimize damage to the cut end.

A semi-circular groove was milled in each of the two plates along their lengths. The diameter of this groove was 0.198 cm (0.078 in) while the diameter of the rod was 0.193 cm (0.076 in). This provided for a close fit between the rod and the grooves. The depth of the grooves were made less than 0.0965 cm (0.038 in) by 0.0127 cm (0.005 in)  $\pm$  0.005 cm (0.002 in). The purpose of this was to insure that when the two plates sandwiched the rod in the grooves, it would be compressed by the entire surface of the grooves. The grooves of the two plates were aligned so that the rod would fit snugly between them forming a circular clamp. Four machine screws placed in a square pattern were used to provide the clamping force. (Refer to Figs. A-4, A-5, A-6, and A-7 for a better idea of the set-up.) A pin was pressed into the lower plate to allow accurate alignment of the upper plate. A saw slot was cut through the top plate and deep enough into the bottom plate to insure that the rod was cut. This slot was placed right between the four screws with two screws on either side.

As shown in Figs. A-6 and A-7, a dial indicator was used as part of the set-up to aid in the accuracy of the

length cuts. This helped to keep the rod lengths to within 0.0051 cm of the desired length with relative ease.

Water was applied during cutting and the rate of cutting was approximately 0.06 cm/sec.

To a visual inspection, these cuts appeared smooth and seemed to not disturb the casing because flaring was extremely minimal. Because of the slow rate of cutting and the water coolant, there was no burning detected. The resin on a macroscopic level appeared undisturbed. Further examination under a microscope (50X) showed little evidence of flaring of the rod ends. (See Fig. A-8.)

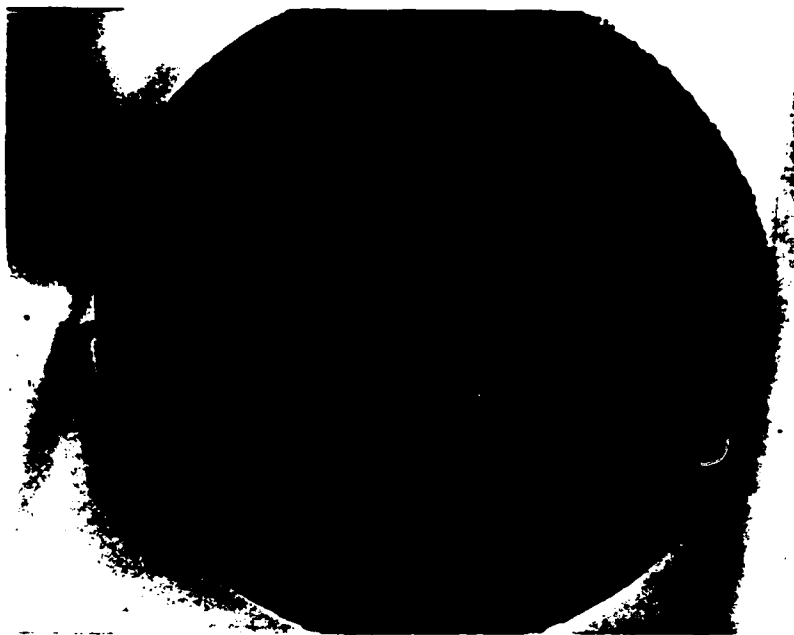


Fig. A-1 Magnification of a rod end cut  
using wax encasement. (50x)



Fig. A-2 Magnification of another rod cut  
using wax encasement. (50x)

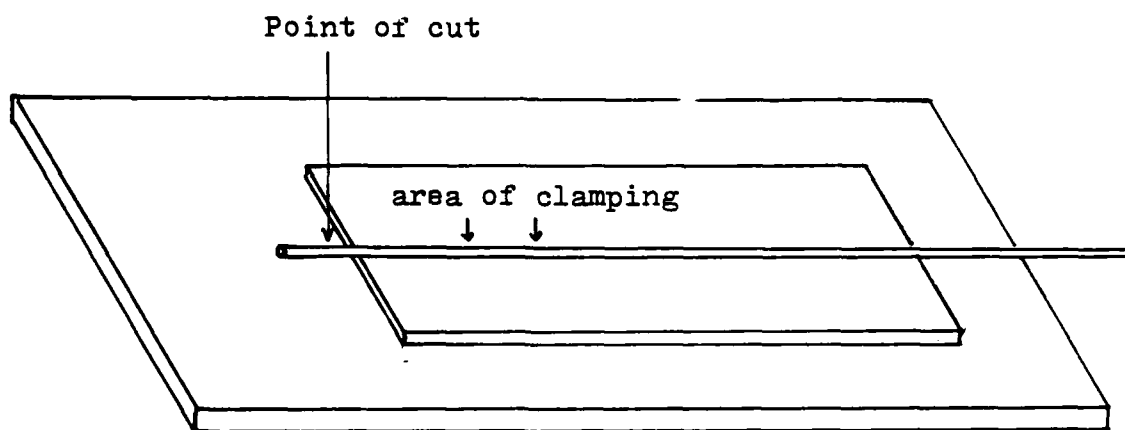


Fig. A-3 Simply supported end cutting.

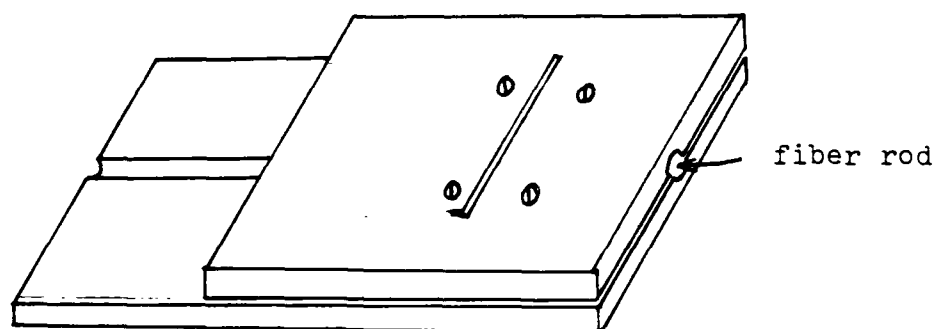


Fig. A-4 Sketch of clamping plates for cutting.



Fig. A-5 Clamping plate disassembled.

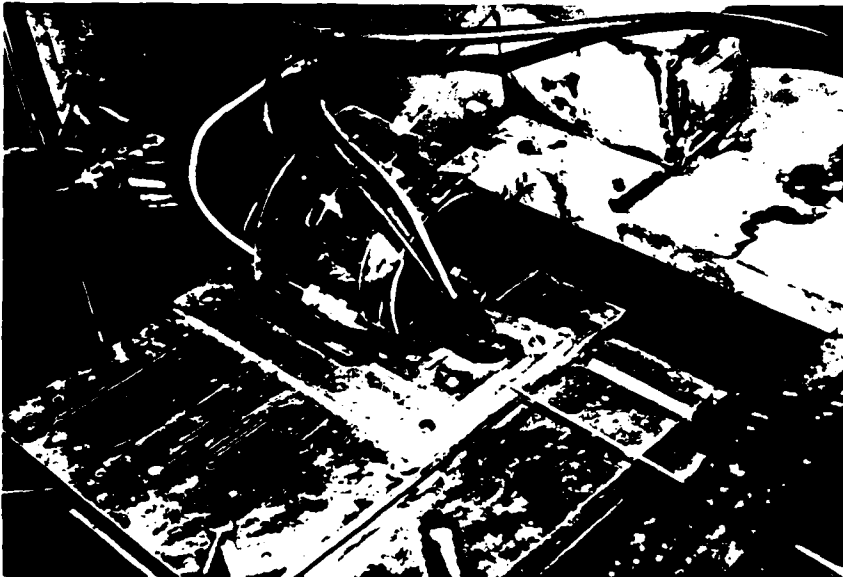


Fig. A-6 Rod cutting set-up.



Fig. A-7 Rod cutting set-up.



Fig. A-8 Representative section of a rod end cut  
using the aluminum plate clamp.

## APPENDIX B

### ULTRASONIC TEST SYSTEM

A schematic of the experimental system is shown in Fig. B-1. The system consists of a pulsed oscillator (Arenberg Model PG-652-C Mod II) for generating single frequency wave packet signals; two transducers (AET Model MAC 300-L, one each for transmission and reception); an attenuator (Arenberg Model ATT-693); a low frequency inductance tuner (Arenberg Model LFT-500); a low frequency amplifier (Arenberg Model LFA-550); an oscilloscope (Tektronix Model 455); a transducer-specimen couplant (AET SC-6), and a set of clamping hair clips to provide reasonably constant force.

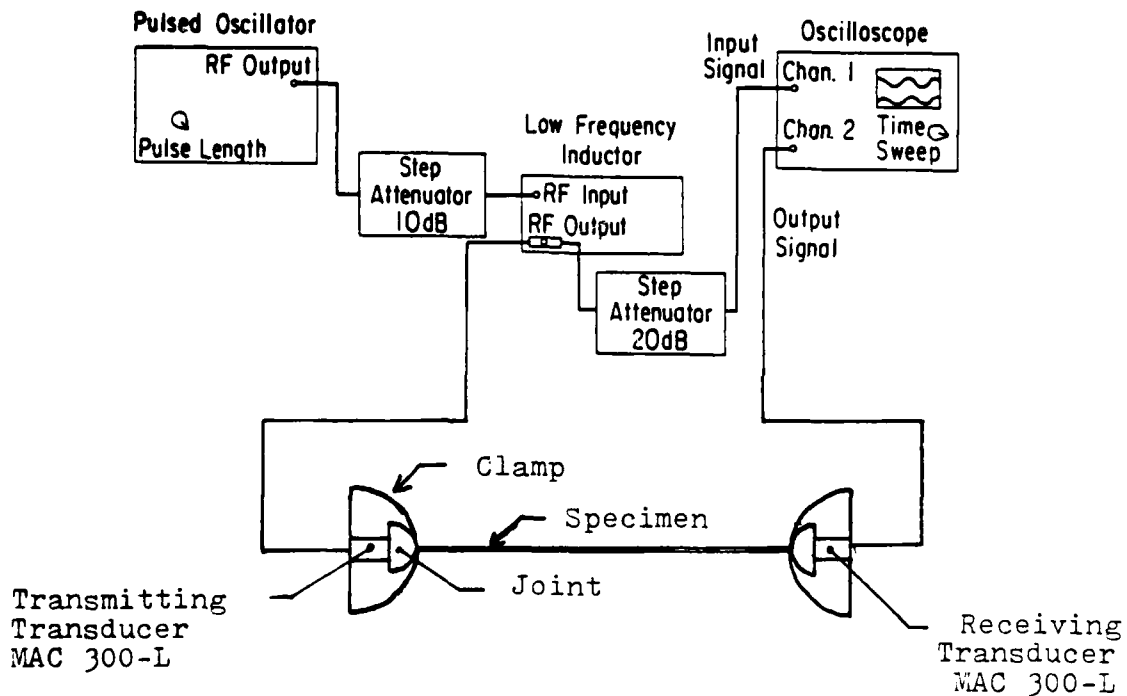


Fig. B-1 Schematic of ultrasonic attenuation test system.

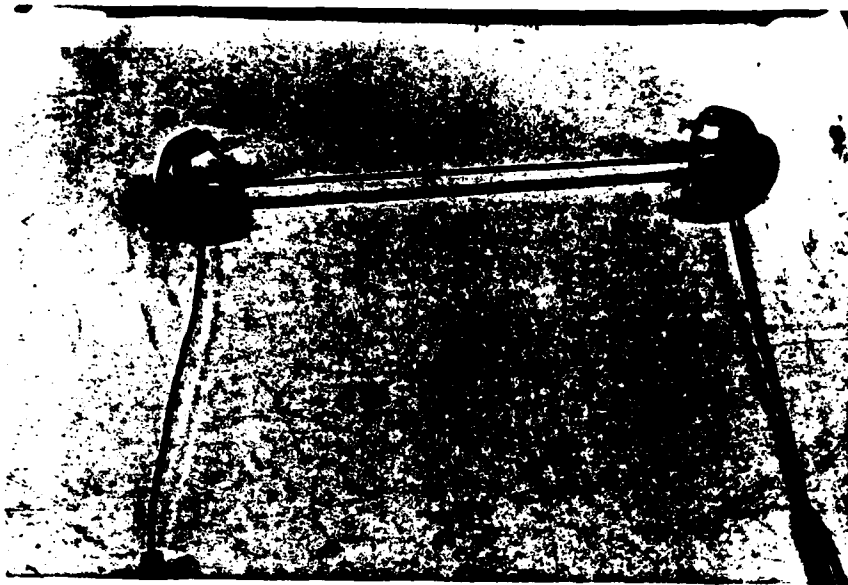


Fig. B-2 Transducers clamped to the ends of a specimen.

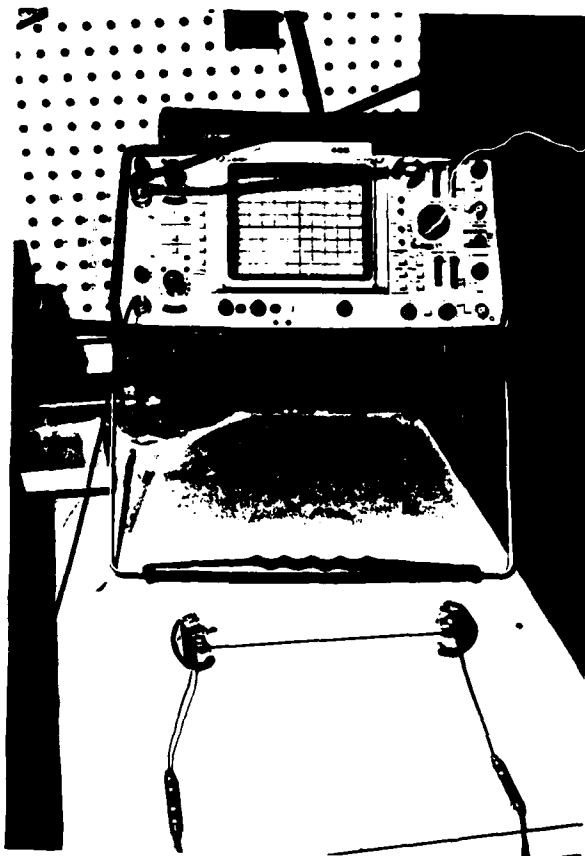


Fig. B-3 Oscilloscope and specimen set-up.

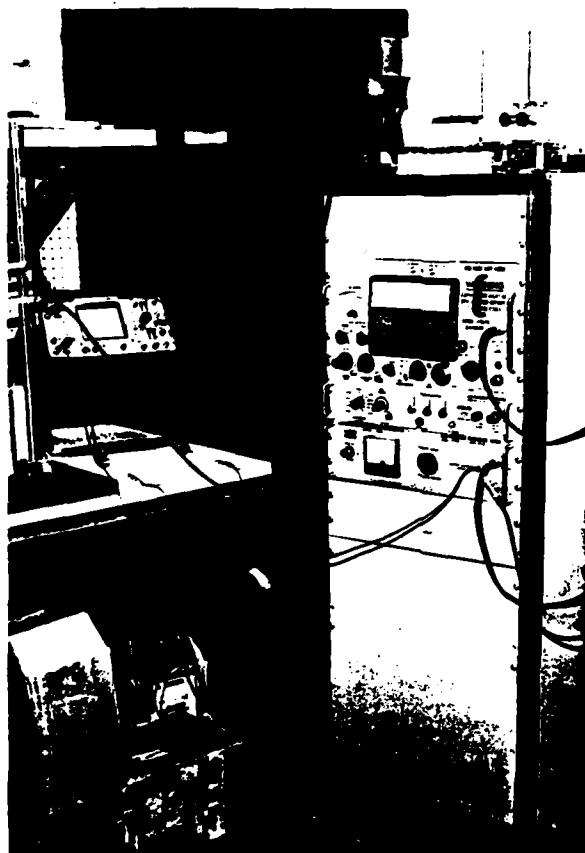


Fig. B-4 Ultrasonic Attenuation Test System.

## APPENDIX C

### DESIGN OF JOINTS FOR THE TETRAHEDRAL TRUSS

The mechanical drawing of the joint received from NASA had the angles for the holes mislabelled. (See Fig. C-7.) Also, the orientation of this joint was meant to enable a tetrahedral truss platform to be constructed with the flat face of the joint parallel to the plane of the platform. The use of this joint for the tetrahedral truss would have introduced asymmetries in the wave propagation characteristics of the model. (i.e., the flat joint faces would not be orthogonal to the structure.) For this reason, the joints were redesigned.

The type A joint was essentially designed to be the apex of a pyramid, with its flat face being parallel to the base of the pyramid and facing away from it. The proper angles of the holes were calculated in the following way: Fig. C-1 shows the oblique projection of a single pyramid. As can be seen, four holes are needed on the lower side of the joint which was made spherical. The angles between the members a, b, c, and d and the vertical centerline of the joint are equal to the angle of CAB which is labelled by F in Fig. C-1. Suppose the members all have unit length,

$$\overline{BC} = \sqrt{\left(\frac{1}{2}\right)^2 + \left(\frac{1}{2}\right)^2} = \sqrt{\frac{1}{2}}$$
$$F = \sin^{-1} \frac{\overline{BC}}{\overline{AC}} = \sin^{-1} \sqrt{\frac{1}{2}} = 45^\circ$$

The angles between any two slanted members are  $90^\circ$  when viewed from the top since the diagonals of a square

intersect at right angles. (See Fig. C-2.) Also shown are two extra members extending to neighboring pyramids. The projection angles of these members are  $45^\circ$  with respect to members a, b, c and d. (i.e., bisectors of right angles.)

The type B joint was designed to have its flat face orthogonal to one member of the tetrahedron. The true angles of members a, b, c and d with respect to the vertical are the true angle of G. (Refer to Fig. C-3) Suppose again that a, b, c, d and e have unit length. (See Fig. C-4 for G'.)

$$\text{The true angle } G' = \sin^{-1} \frac{\overline{BC}}{\overline{AC}} = \sin^{-1}(\frac{1}{2}) = 30^\circ$$

The projection angle between a and be is equal to B in Fig. C-3.

$$B = 2C$$

$$C = \cot^{-1} \frac{1}{\frac{1}{2}} = \cot^{-1} 21$$

Where

$$1 = \frac{\sqrt{2}}{2},$$

giving,

$$C = \cot^{-1} \sqrt{2} = 35.264^\circ$$

Thus,

$$B = 70.529^\circ$$

The projection angles between the members a, b, c and d and the members extending to neighboring tetrahedrons (See Fig. C-3, Front view) from the type B joints are equal to X.

$$X = \frac{180 - B}{2} = 54.736^\circ$$

The mechanical drawings of joint types A and B are in Figs. C-5 and C-6, respectively.

With these modifications, the joints had their flat faces parallel to the plane formed by the joints  $\pm 90^\circ$  away in the structure. This was for ultrasonic testing purposes.

The structure was to be built with a slenderness ratio of 100 with respect to the center of the joints, so the joints had to be 19.3 cm. apart at their centers. The spherical surface of the joints had a larger radius than the cylindrical surface of the joints. The holes were drilled 0.254 cm (0.1 in) deep from the surface, which caused the bottoms of the holes to be different distances from the center of the joint (i.e., its spherical center one). This difference necessitated the cutting the rods to two lengths. The lengths were determined in the following manner.

$$(\text{Distance between Centers}) - (\text{Diameter of } \begin{matrix} \text{Spherical Surface} \\ \text{or} \\ \text{Cylindrical One} \end{matrix})$$

$$+ 2 (\text{Depth of Hole}) = \text{The lengths necessary}$$

$$(19.3 \text{ cm}) - (1.08) + (2)0.254 = 18.74 \text{ cm}$$

$$(19.3 \text{ cm}) - (1.12) + (2) 0.254 = 18.69 \text{ cm}$$

The necessary lengths were 18.74 cm (7.376 in) and 18.69 cm (7.36 in).

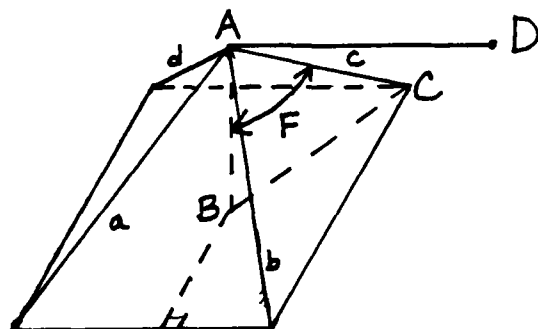


Fig. C-1 Oblique view  
of Pyramid

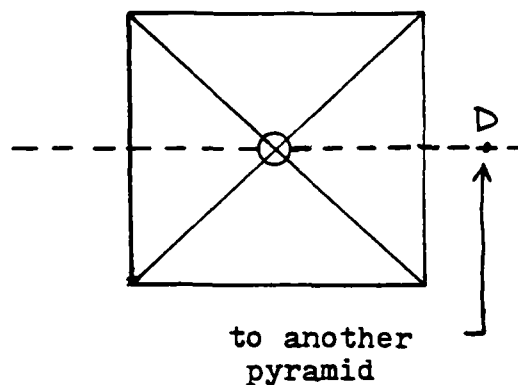
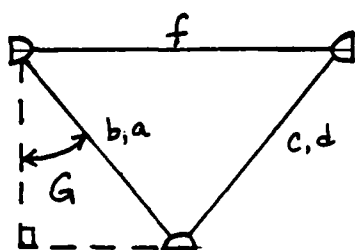
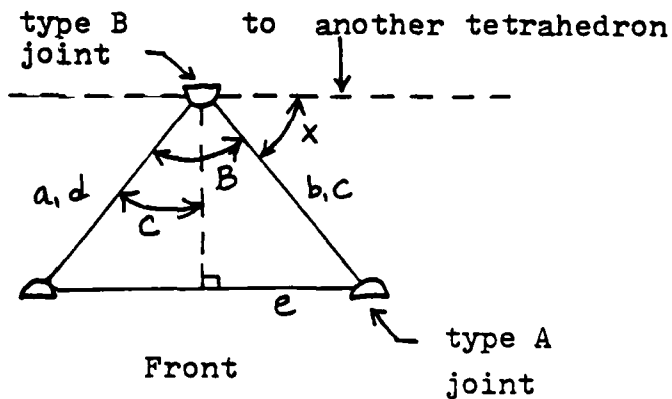


Fig. C-2 Top view  
of Pyramid



Side



Front

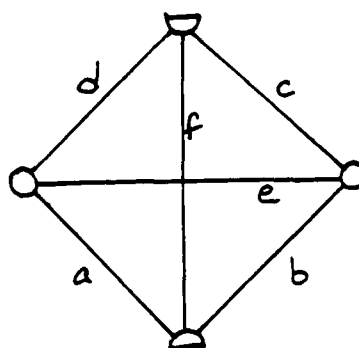


Fig. C-3 First Angle Projection of the Tetrahedron



A vertical strip of five film frames. Each frame shows a dark, grainy image with a small, bright, rectangular object in the center. The object appears to be a small, glowing rectangle, possibly a piece of paper or a small object, against a dark background. The frames are arranged vertically, with the top frame showing the object at the top and the bottom frame showing it at the bottom. The object is slightly tilted and has a soft glow around it. The background is dark and textured, suggesting a film or a dark surface. The frames are separated by thin white lines, and the overall image has a vintage, grainy quality.

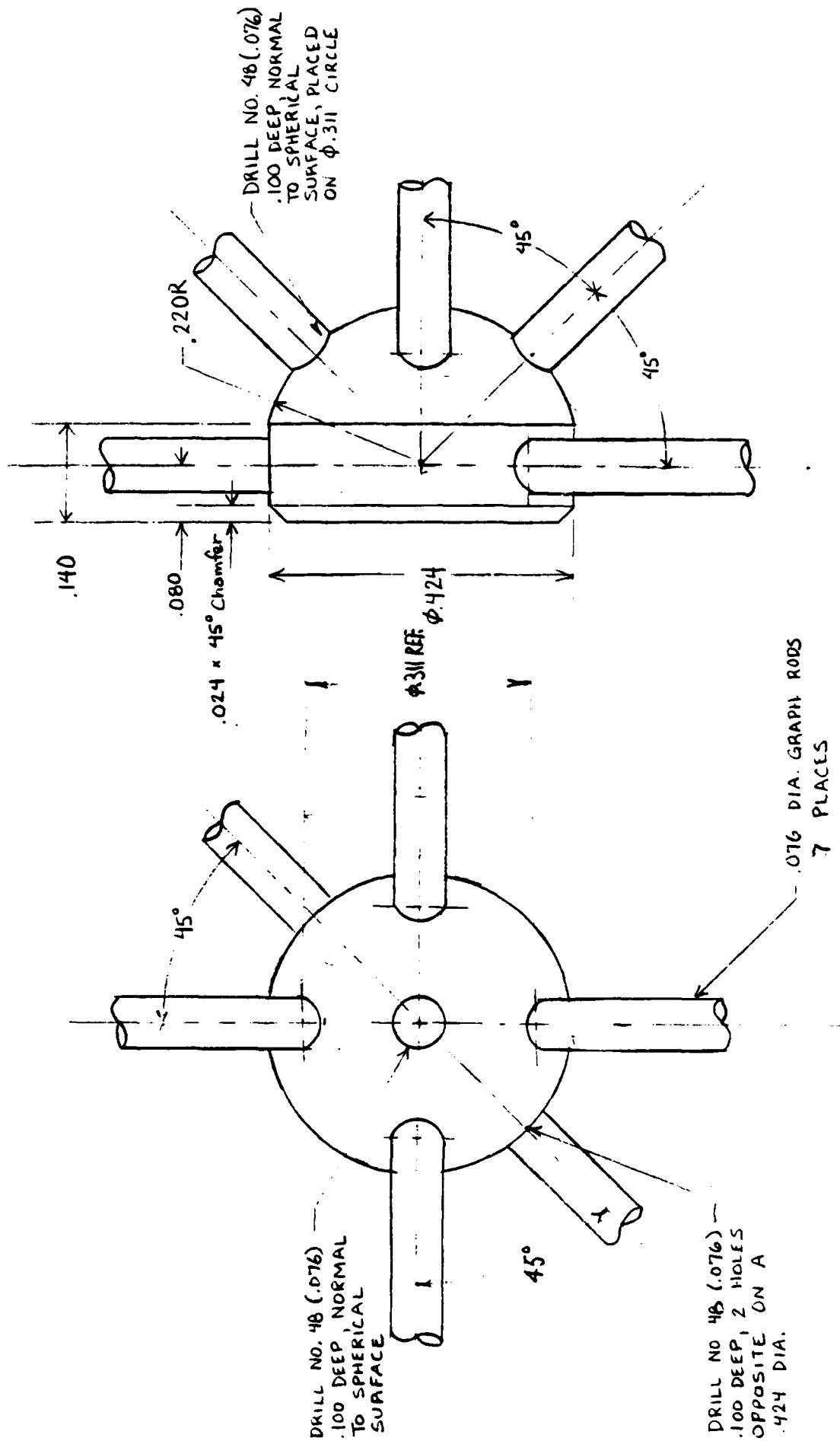


Fig. C-5 Mechanical Drawing of Joint A.

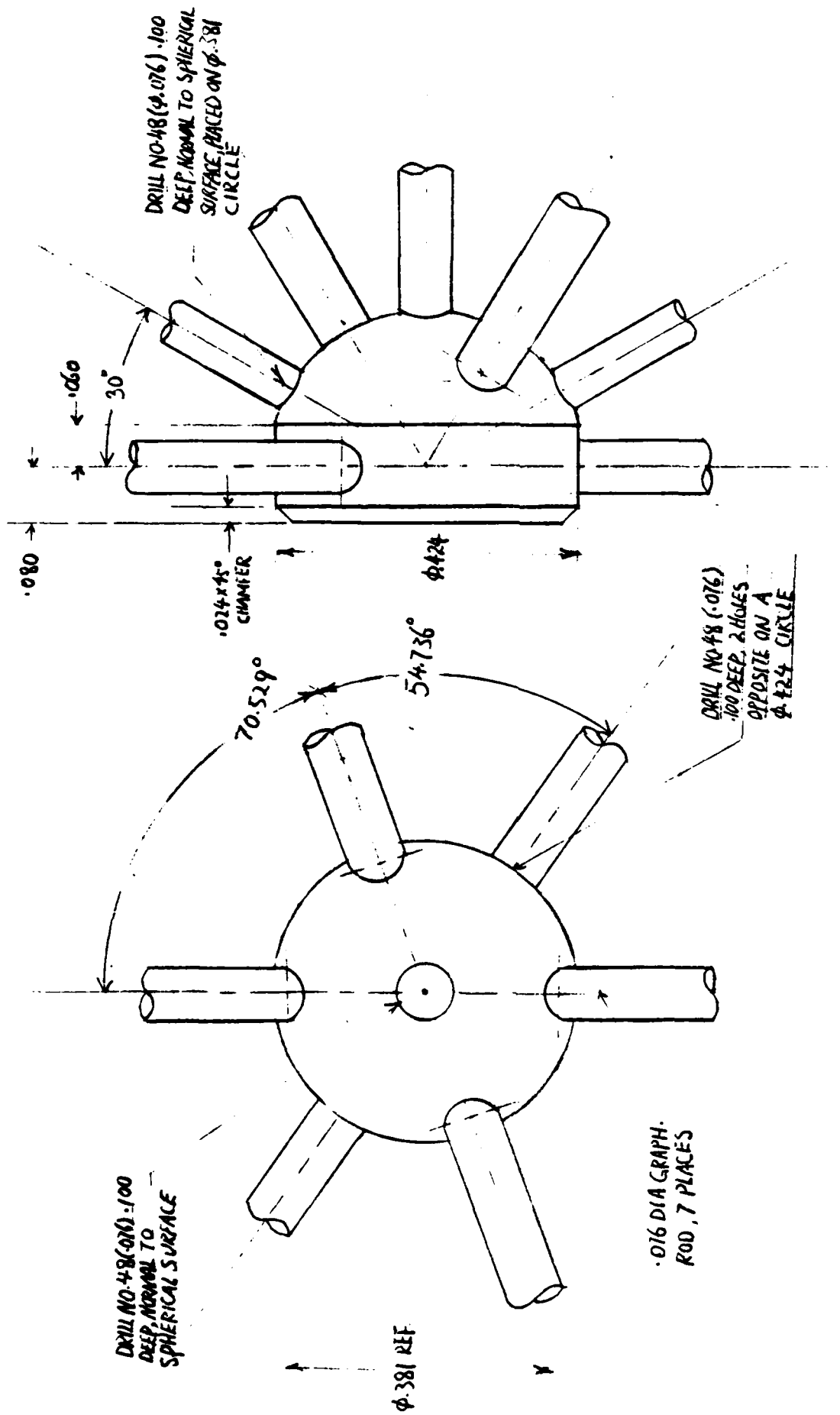


Fig. C-6 Mechanical Drawing of Joint B.

.160

.080

.220 R

.024 x 45° CHAMFER

DRILL NO. 48 ( $\phi .076$ ), 100.  
DEEP, 3 HOLES NORMAL TO  
SPHERICAL SURFACE, EQUALLY  
SPACED ON  $\phi .220$  CIRCLE

30° TYP.

$\phi .400$

$\phi .220$   
REF

30°

30°

DRILL NO. 48 ( $\phi .076$ ), 100 DEEP  
6 HOLES EQUALLY SPACED AROUND  
.400 DIA.

.006 DIA. GRAPH RODS  
9 PLACES, REF.

Fig. C-7 Mechanical Drawing of Joint from NASA.

## APPENDIX D

### CHARACTERIZATION DATA OF JOINTS AND RODS USED IN THE STRUCTURES

As stated earlier, the joints and rods used in the structures were measured and examined before their use. What follows is the information produced for these structures.

#### Single rod with two joints

Specimen #1 - 1 rod, length 18.69 cm, 1.09 g  
2 type B joints, weight of each was 1.33g,  
diameter of each was 1.08 cm, and their  
heights were 0.766 cm.

Specimen #2 - 1 rod, length 18.69 cm, 1.08 g  
2 type A joints, both with weights of  
1.39 g, diameter of 1.08 cm, and heights  
of 0.772 cm.

TABLE D-1

## TETRAHEDRON CHARACTERIZATION DATA

<u>Specimen Number</u>	<u>Element</u>	<u>Type</u>	<u>Weight (grams)</u>	<u>Diameter (cm)</u>	<u>Height (cm)</u>	<u>Length (cm)</u>
1	Joint (1)	A	1.36	1.08	0.768	---
	Joint (1)	A	1.36	1.08	0.764	---
	Joint (1)	B	1.33	1.08	0.762	---
	Joint (1)	B	1.33	1.08	0.764	---
	Rod (1)	-	1.09	0.193	---	18.735
	Rod (5)	-	1.09	0.193	---	18.694
2	Joint (1)	A	1.39	1.08	0.771	---
	Joint (1)	A	1.39	1.08	0.771	---
	Joint (1)	B	1.35	1.077	0.767	---
	Joint (1)	B	1.35	1.077	0.767	---
	Rod (1)	-	1.09	0.193	---	18.735
	Rod (4)	-	1.08	0.193	---	18.694
	Rod (1)	-	1.09	0.193	---	18.694
3	Joint (1)	A	1.36	1.077	0.764	---
	Joint (1)	A	1.36	1.08	0.762	---
	Joint (1)	B	1.34	1.077	0.767	---
	Joint (1)	B	1.34	1.08	0.770	---
	Rod (1)	-	1.09	0.193	---	18.735
	Rod (5)	-	1.08	0.193	---	18.694

TABLE D-2  
PYRAMID CHARACTERIZATION DATA

<u>Specimen Number</u>	<u>Element (quantity)</u>	<u>Type</u>	<u>Weight (grams)</u>	<u>Diameter (cm)</u>	<u>Height (cm)</u>	<u>Length (cm)</u>
1	Joint (1)	A	1.39	1.08	0.770	---
	Joint (1)	B	1.32	1.08	0.759	---
	Joint (1)	B	1.32	1.087	0.759	---
	Joint (1)	B	1.32	1.077	0.762	---
	Joint (1)	B	1.32	1.082	0.757	---
	Rods (2)	-	1.09	0.193	---	18.735
	Rods (6)	-	1.08	0.193	---	18.694
2	Joint (1)	A	1.36	1.08	0.764	---
	Joint (1)	B	1.34	1.077	0.770	---
	Joint (1)	B	1.34	1.08	0.762	---
	Joint (1)	B	1.34	1.08	0.764	---
	Joint (1)	B	1.34	1.08	0.770	---
	Rods (2)	-	1.09	0.193	---	18.735
	Rods (6)	-	1.08	0.193	---	18.694
3	Joint (1)	A	1.36	1.08	0.764	---
	Joint (1)	B	1.34	1.08	0.764	---
	Joint (1)	B	1.34	1.08	0.764	---
	Joint (1)	B	1.34	1.08	0.767	---
	Joint (1)	B	1.34	1.08	0.767	---
	Rods (2)	-	1.09	0.193	---	18.735
	Rods (6)	-	1.09	0.193	---	18.694

## APPENDIX E

### ORIENTATION AND LABELLING OF THE BASIC STRUCTURES

The joints of the tetrahedrons and the pyramids were labelled because of their differing orientations and the desire to characterize each of them. Figs. E-1 and E-2 are photographs of the tetrahedrons.

The tetrahedrons were oriented by a piece of paper taped to one rod. On the paper was written the specimen's number in large print and to either side of this were the numbers 1 and 2. The numbers 1 and 2 identified which joints were subsequently identified as joints 1 and 2, respectively. By placing one's right hand around the rod with the piece of paper and pointing the thumb towards joint 2, the fingers will first cross joint 3 and then joint 4. (See Fig. E-3).

The identification paper was always fastened to a rod with two joints that had their flat faces orthogonal to the rod.

The pyramid was set on its square base and the apex was called joint 1. (See Figs. E-4 and E-5 for the orientation of the pyramids.) The identification paper was attached as shown in Fig. E-6 and the joint attached to the rod was labelled number 2 (not including joint 1). Looking down on the pyramid, joints 3, 4 and 5 were labelled clockwise in order.

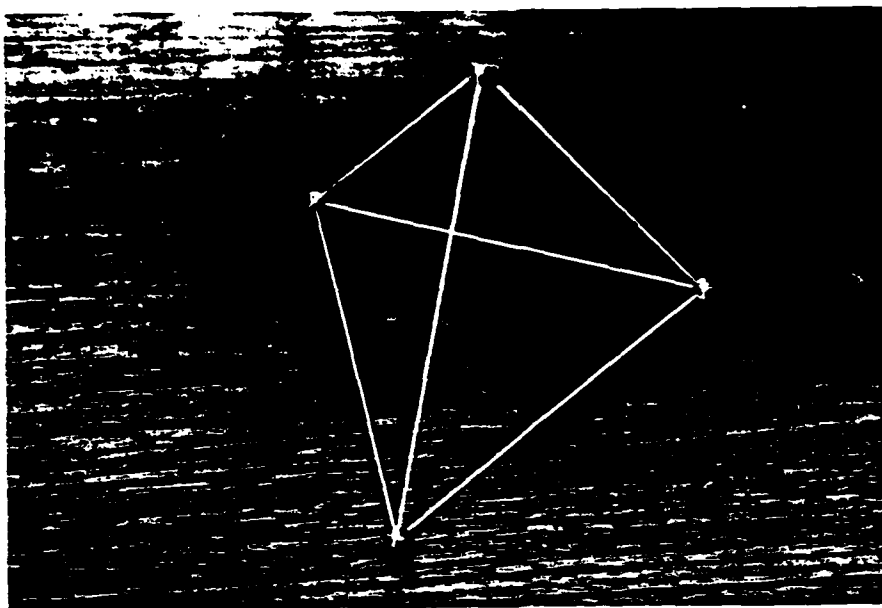


Fig. E-1 Typical Tetrahedron.

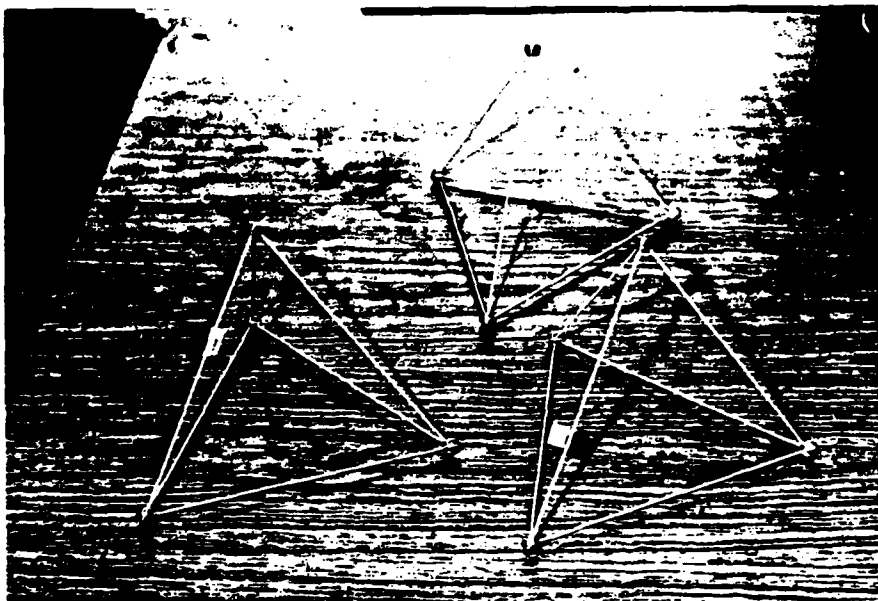


Fig. E-2 Test Tetrahedrons.

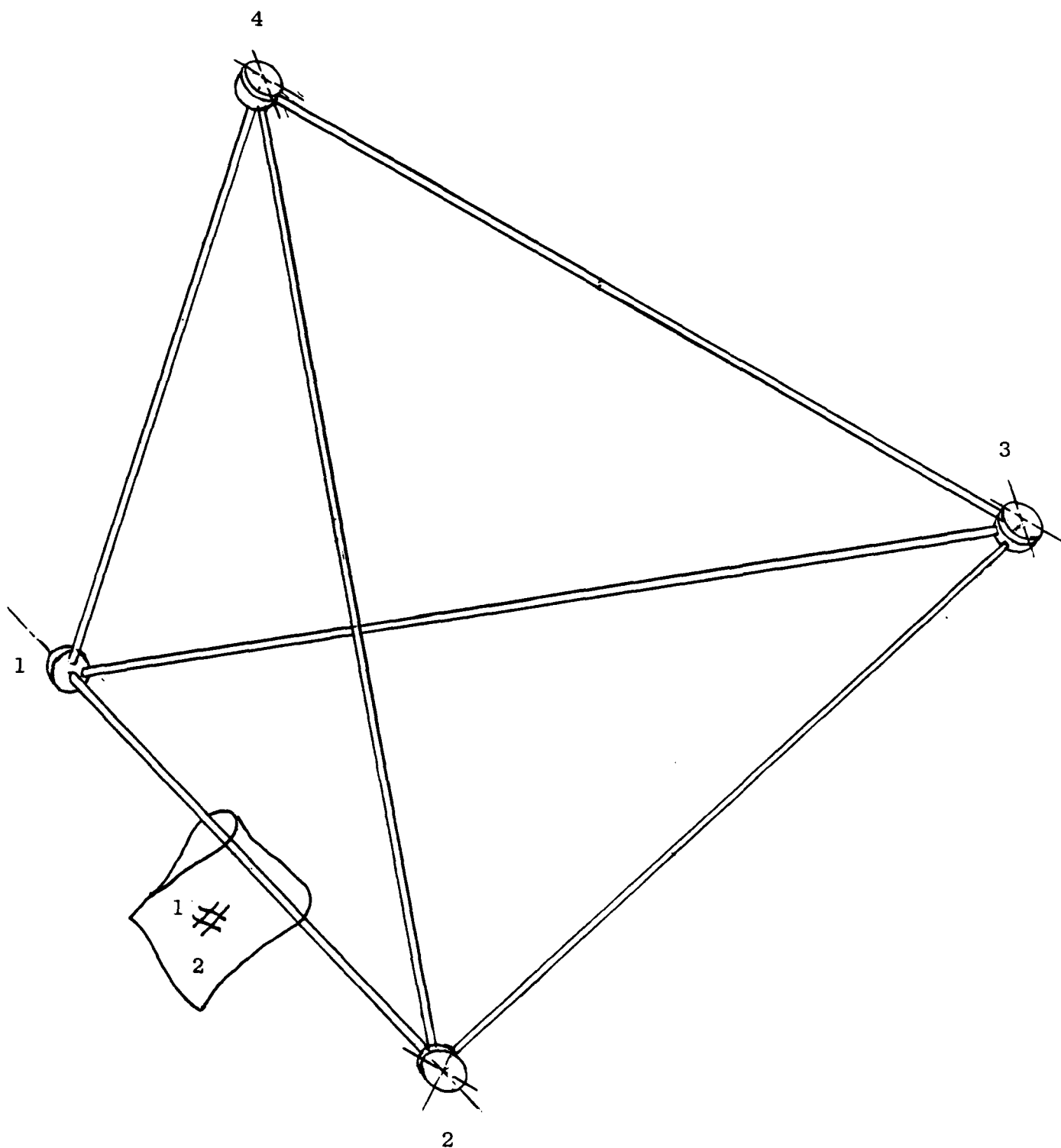


Fig. E-3 Orientation and Labelling of the Tetrahedrons

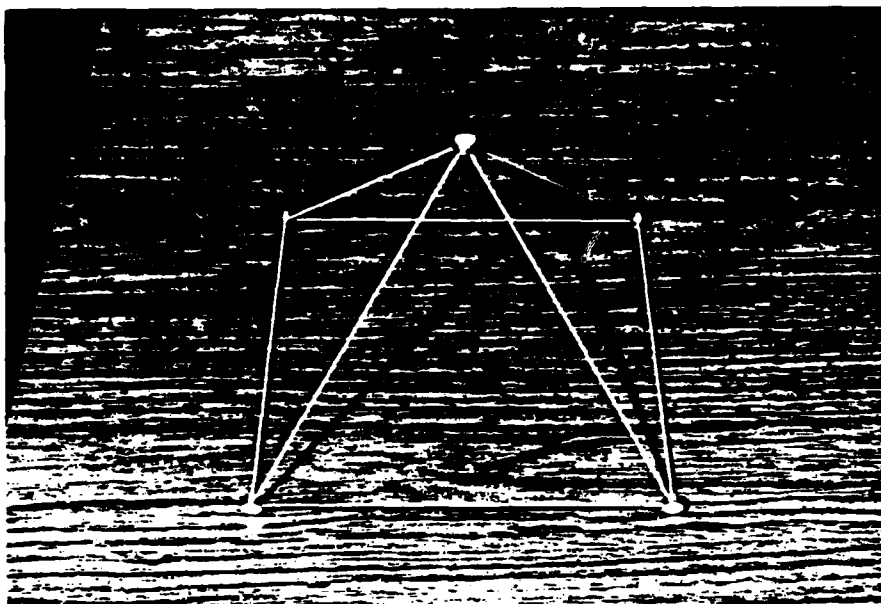


Fig. E- 4 Typical Pyramid.

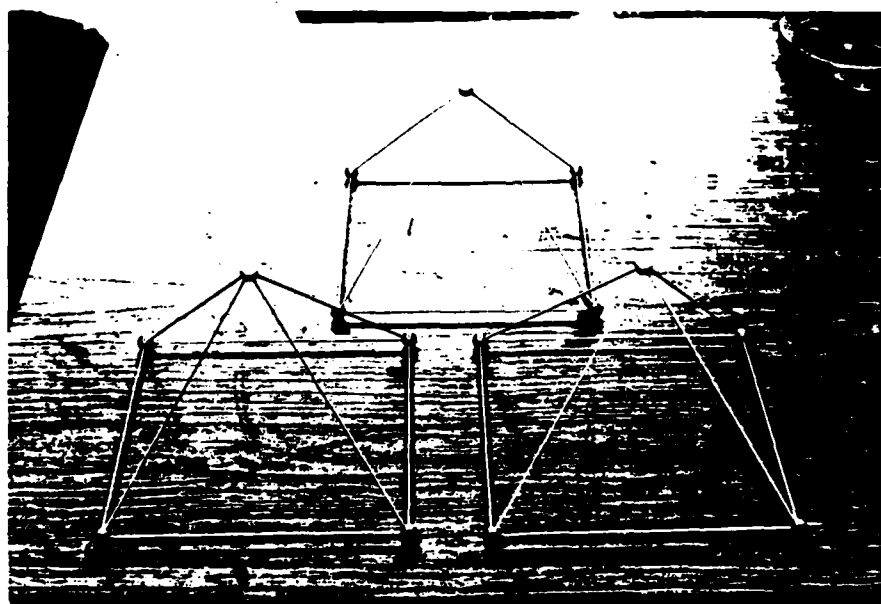


Fig. E-5 Test Pyramids.

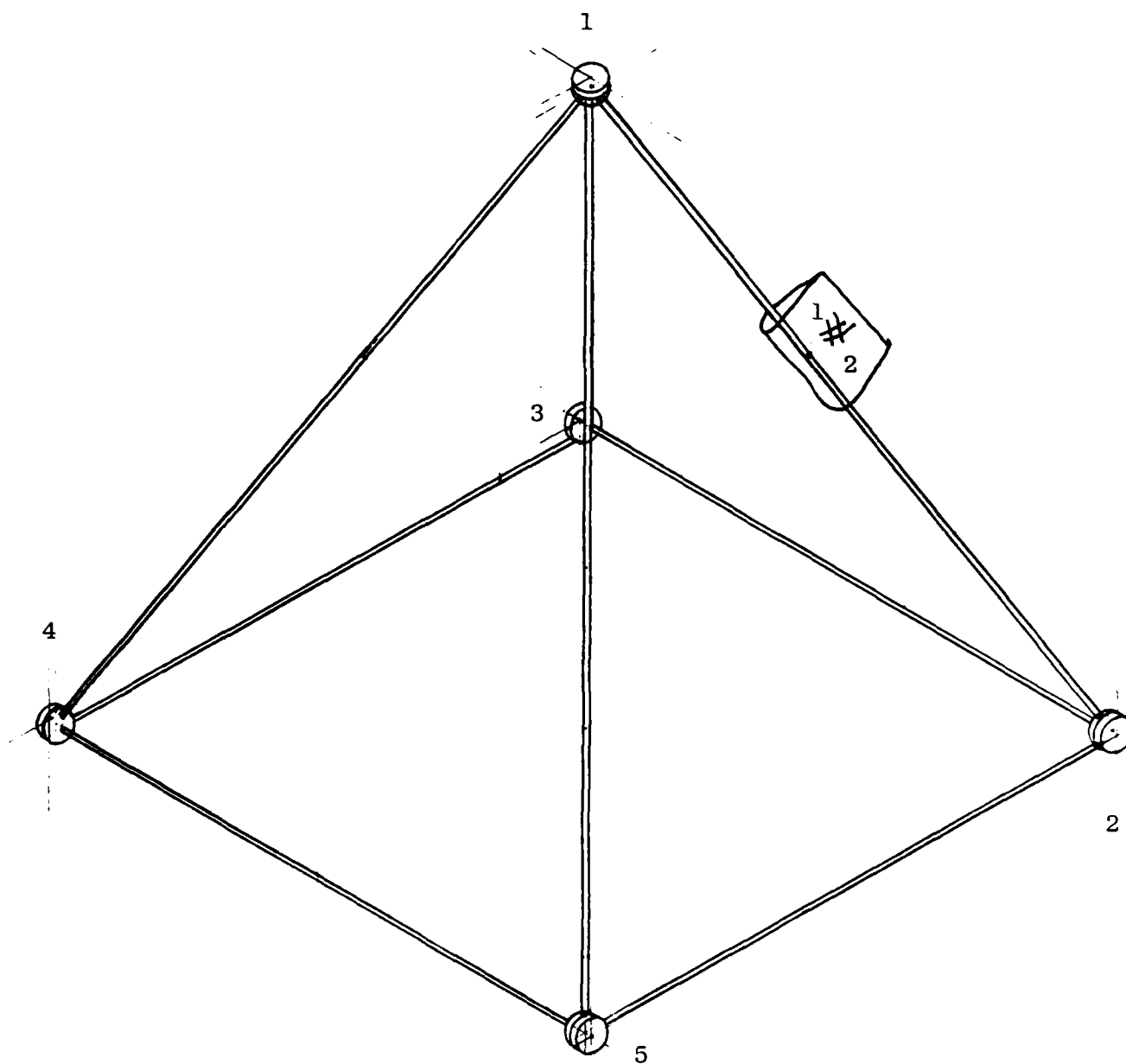


Fig. E-6 Orientation and Labelling of the Pyramid.

**END**

**FILMED**

*2-86*

**DTIC**